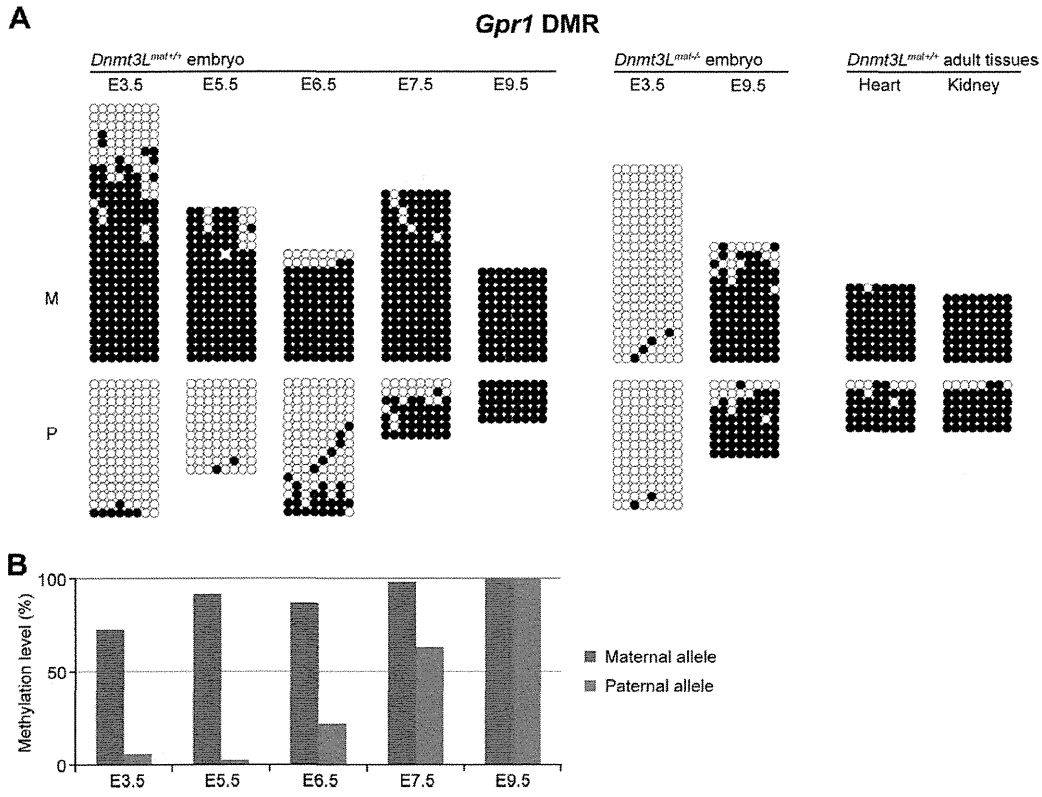

Fig. 2. DNA methylation profile of the *Gpr1* DMR. (A) Bisulfite sequencing analysis of the *Gpr1* DMR in wild-type and *Dnmt3L*$^{mat-/-}$ mouse embryos and adult tissues. Each row of circles represents the results of an independent sequencing reaction. The open and closed circles denote unmethylated and methylated CpGs, respectively. M and P indicate the maternally inherited B6 or 129 × B6 alleles and the paternally inherited JF allele, respectively. Both alleles were discriminated by three polymorphisms [23]. (B) Differential methylation status between M and P alleles during embryogenesis. CpG methylation levels of maternal and paternal alleles are represented by red and blue bars, respectively. These histograms were obtained from bisulfite sequencing analyses shown in (A).

ylated *Gpr1* DMR lost its mono-allelic methylation during gastrulation. To explain the apparent contradiction of the *Gpr1* DMR methylation status being unassociated with the imprinted expression of either the *Zdbf2* or *Gpr1* genes, we focused on a long intergenic non-coding RNA (lincRNA) located within the *Gpr1-Zdbf2* locus (Fig. 3A). This 114-kb lincRNA, which we named *Zdbf2linc*, had previously been identified in mouse ES cells by massively parallel cDNA sequencing (RNA-seq) and chromatin immunoprecipitation sequencing (ChIP-seq) [30]. *Zdbf2linc* is a splice variant of *Zdbf2* that contains seven exons, including three unique exons within intron 2 of the *Gpr1* gene (exon A and B), the *Gpr1/Zdbf2* intergenic region (exon C), and exons 3, 4, 6, and 7 of the *Zdbf2* gene (according to NCBI RefSeq). A long-range splice form of *Zdbf2linc* lacking exon C was also identified in ES cells by 5′ rapid amplification of cDNA ends (RACE) (Fig. 3A). Interestingly, the transcription start site of *Zdbf2linc* overlaps the *Gpr1* DMR. To determine if *Zdbf2linc* is detectable in vivo and is imprinted, we performed RT-PCR and allelic expression analysis in early to mid-term mouse embryos. *Zdbf2linc* expression was detected from E3.5 to E7.5 (Fig. 3B and C), during which time paternal-allele-specific expression was observed (Fig. 3D). Quantitative RT-PCR showed higher expression of *Zdbf2linc* than that of the original *Zdbf2* coding variant (including exon 5) in blastocysts and ES cells (Fig. 3C). Although *Zdbf2linc* was undetectable at E9.5, the expression of the original *Zdbf2* variant was clearly detected (Fig. 3B). Interestingly, the timing of *Zdbf2linc* repression was nearly identical to that of the loss of the differential methylation of the *Gpr1* DMR. Furthermore, *Dnmt3L*$^{mat-/-}$ embryos showed biallelic expression of *Zdbf2linc*. These findings indicate that methylation at *Gpr1* DMR may directly repress *Zdbf2linc* expression in *cis*.

3.4. Erasure and re-establishment of paternal-allele-specific methylation at Zdbf2 DMRs

While the methylation of *Gpr1* DMR and *Zdbf2linc* expression were correlated in *cis*, the epigenetic regulation of the original *Zdbf2* variant, which is expressed exclusively from the paternal allele after the E9.5 stage (Fig. 3B), remains unclear. We therefore investigated the methylation patterns of the *Zdbf2* DMRs present in the intragenic region of *Zdbf2linc*. All DMRs showed male-germ-cell specific hypermethylation in previous studies [21–23] and paternal-allele-specific hypermethylation in E9.5 embryos in this study (Fig. 4 middle); however, our previous DNA methylome analyses have shown that *Zdbf2* DMRs are deeply undermethylated in blastocysts [23]. Allelic methylation analyses performed in this study further confirmed that both the paternal and maternal alleles are unmethylated at the *Zdbf2* DMR3 in blastocysts (Fig. 4 left). Taken together, our results demonstrate that paternal-allele-specific methylation of the *Zdbf2* DMRs established in germ cells are erased after fertilization and re-established after implantation. Interestingly, biallelic hypermethylation of the *Zdbf2* DMRs was observed in *Dnmt3L*$^{mat-/-}$ embryos at E9.5 (Fig. 4 right), which is similar to the methylation pattern observed for the somatic DMR (*Nesp* DMR) in the imprinted *Gnas* cluster [17]. This suggests that not only are the *Zdbf2* DMRs in the intragenic region of *Zdbf2linc* somatic (secondary), but that the methylation of *Zdbf2* DMRs is

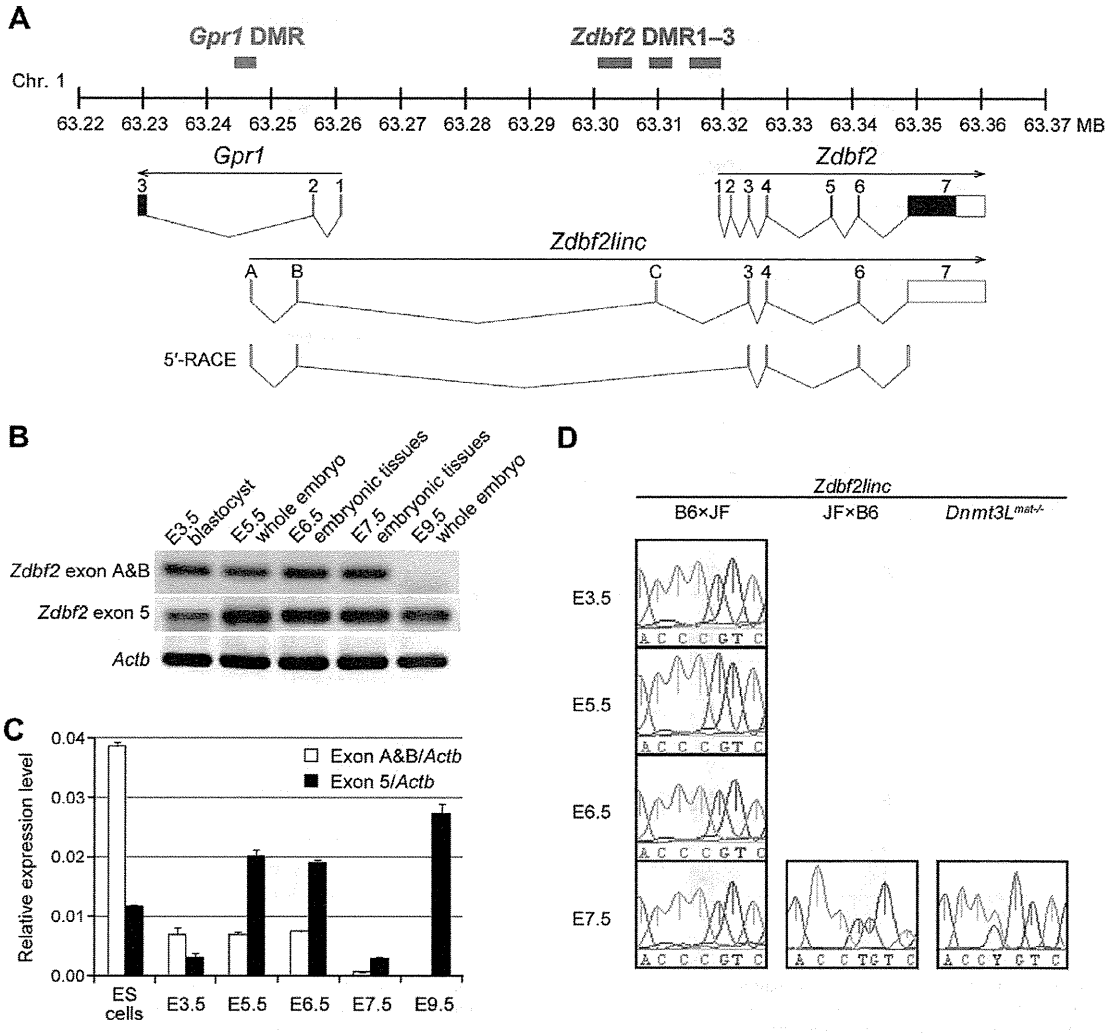

Fig. 3. Quantitative and allelic-specific expression analyses of *Zdbf2linc*. (A) Schematic physical map of the imprinted *Gpr1-Zdbf2* domain showing three paternally expressed transcripts and the 5′-RACE sequence. Red and blue bars represent maternally or paternally methylated DMRs, respectively. (B) Expression of two variants of *Zdbf2* during embryonic development. Forty cycles of RT-PCR were carried out for exon A/B and exon 5 of the *Zdbf2* gene (no SNPs were present) and *Actb* (as a control). (C) Quantitative RT-PCR analysis using the same primers as for (B) in ES cells and individual stage embryos. Expression levels of transcripts were normalized to those of the *Actb* gene. Error bars represent SEM ($n = 3$). (D) Allelic expression analysis of *Zdbf2* was performed using reciprocal F_1 hybrid embryos (B6 × JF and JF × B6), and embryos produced by mating between *Dnmt3L*-deficient females and JF males ($Dnmt3L^{mat-/-}$). Maternal and paternal alleles were distinguished by a SNP in exon A (C/T at chr1. 63,247,248; highlighted in yellow).

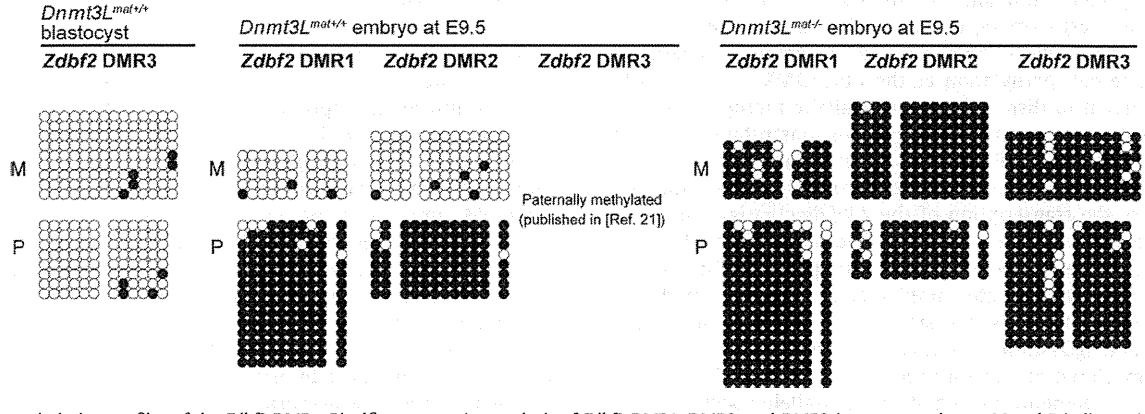

Fig. 4. DNA methylation profiles of the *Zdbf2* DMRs. Bisulfite sequencing analysis of *Zdbf2* DMR1, DMR2, and DMR3 in mouse embryos. M and P indicate the maternally inherited (B6 or 129 × B6) and paternally inherited (JF) alleles, respectively.

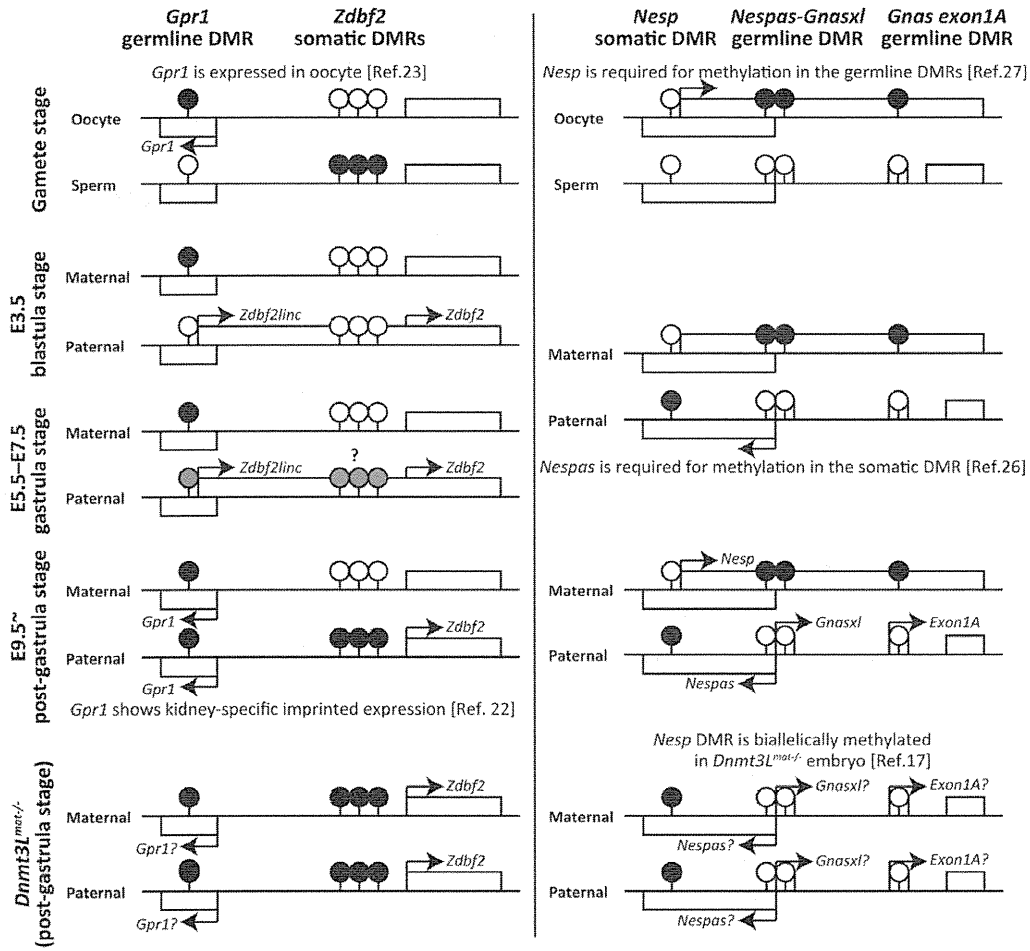

Fig. 5. Summary of allele-specific epigenetic and gene expression differences within the *Gpr1-Zdbf2* (left) and *Gnas* (right) loci. Open boxes represent the locations of the individual imprinted genes (or alternative promoter/first exons); arrows represent the transcriptional direction of these genes. The positions of the DMRs are indicated by filled and unfilled pins on the methylated and unmethylated alleles, respectively. Grey-filled pins indicate the partial methylated CpGs.

positively correlated to the expression of the original *Zdbf2* variant in *cis* after gastrulation.

4. Discussion

We identified a novel, long, imprinted, non-coding variant of the *Zdbf2* gene, *Zdbf2linc*, which is transcribed from the *Gpr1* DMR during the blastula and gastrula stages of mouse embryonic development. Furthermore, we found the paternal-allele-specific expression of *Zdbf2linc* to be negatively correlated with germline-derived maternal methylation at the *Gpr1* DMR. The *Gpr1* DMR was also shown to display complete biallelic methylation, while *Zdbf2linc* was rarely expressed in the post-gastrulation. It is unknown why the *Gpr1* DMR becomes hypermethylated after gastrulation; however, our results indicate that methylation at this DMR may repress the transcription of the *Zdbf2linc* variant in *cis*. The *Zdbf2* DMRs located within the transcribed region of *Zdbf2linc* were also shown to be secondary DMRs, with paternal-allele-specific methylation established after implantation. The imprinted *Gpr1-Zdbf2* locus therefore has two similarities with the *Gnas-Nespas*, *Kcnq1ot1*, and *Igf2r-Airn* imprinted clusters: (i) two differential states of imprinted methylation; namely, maternal-allele-specific methylation at gametogenesis and paternal-allele-specific methylation after fertilization, and (ii) transcription of long non-coding RNAs from each maternally methylated primary DMR (Fig. 5). Recently, lincRNAs have become a new paradigm for gene regulation via chromatin remodeling in a variety of biological processes, including events during embryonic development such as X chromosome dosage compensation [31,32], regulation of *Hox* genes [33], or genomic imprinting. The non-coding RNAs of the well-studied imprinted clusters *Nespas*, *Kcnq1ot1*, and *Airn* repress neighboring genes in *cis* [24–26], suggesting that the transcription of imprinted *Zdbf2linc* may also have a similar *cis*-regulating effect on flanking genes.

Allele-specific expression analyses using the heterozygous offspring of homozygous *Dnmt3L*-deficient females demonstrated that the imprinted expression of both *Zdbf2linc* and the original *Zdbf2* variant are subject to maternal methylation imprinting, whereby the original *Zdbf2* variant maintains paternal-allele-specific expression even after the gastrula stage, and *Zdbf2linc* and *Gpr1* DMR imprinting loss occurs. It is also possible that another mono-allelic epigenetic modification may become established via long-range transcription of *Zdbf2linc*, or that paternal-allele-specific methylation of *Zdbf2* DMRs may arise through the methylation of a transcribed region of *Zdbf2linc*. Some studies have also suggested that histone modifications at imprinted domains are a prerequisite for DNA methylation. Transcription across DMRs has been shown to be associated with histone methylation changes and the acquisition of genomic imprinting [26,27,34]. For example,

Williamson et al. have shown that paternally expressed non-coding *Nespas* transcription is required for the demethylation of trimethylated histone H3 lysine 4 (H3K4), followed by DNA methylation at the somatic *Nesp* DMR [26]. *Zdbf2linc* has also been identified as a lincRNA on the basis of the trimethylation states of H3K4 at its promoter region and histone H3 lysine 36 (H3K36) along its transcribed region, at least in ES cells [30]. Finally, the interaction of DNMT3A with chromatin is inhibited by H3K4 methylation [35], but promoted by H3K36 methylation [36]. Histone modifications may therefore control imprinted gene expression prior to allele-specific DNA methylation [5].

The imprinted *Gpr1-Zdbf2* locus also has features distinct from those of other imprinted loci. For instance, the primary *Gpr1* DMR does not maintain its mono-allelic methylation after fertilization, while the secondary *Zdbf2* DMRs are differentially methylated, even during gametogenesis. Furthermore, only paternally expressed transcripts were identified in the *Gpr1-Zdbf2* cluster, whereas the majority of imprinted clusters comprise both maternally and paternally expressed genes. Although the true functional roles of the *Gpr1* and *Zdbf2* genes remain unclear, we have herein identified a novel imprinted lincRNA variant of *Zdbf2* expressed exclusively from the paternal allele in the early embryo. Further investigations would elucidate the roles of the imprinted *Gpr1-Zdbf2* locus and its lincRNA variants in the control of embryonic growth and development.

Acknowledgment

This work was supported by Grants-in-Aid for Scientific Research from the Ministry of Education, Science, Sports and Culture of Japan (Grant Nos. 222228004, 20062009, 221S0002, S0801025).

References

[1] Reik, W. and Walter, J. (2001) Genomic imprinting: parental influence on the genome. Nat. Rev. Genet. 2, 21–32.
[2] Stoger, R., Kubicka, P., Liu, C.G., Kafri, T., Razin, A., Cedar, H. and Barlow, D.P. (1993) Maternal-specific methylation of the imprinted mouse Igf2r locus identifies the expressed locus as carrying the imprinting signal. Cell 73, 61–71.
[3] Coombes, C. et al. (2003) Epigenetic properties and identification of an imprint mark in the Nesp-Gnasxl domain of the mouse Gnas imprinted locus. Mol. Cell. Biol. 23, 5475–5488.
[4] Lopes, S. et al. (2003) Epigenetic modifications in an imprinting cluster are controlled by a hierarchy of DMRs suggesting long-range chromatin interactions. Hum. Mol. Genet. 12, 295–305.
[5] Bhogal, B., Arnaudo, A., Dymkowski, A., Best, A. and Davis, T.L. (2004) Methylation at mouse Cdkn1c is acquired during postimplantation development and functions to maintain imprinted expression. Genomics 84, 961–970.
[6] Sato, S., Yoshida, W., Soejima, H., Nakabayashi, K. and Hata, K. (2011) Methylation dynamics of IG-DMR and Gtl2-DMR during murine embryonic and placental development. Genomics 98, 120–127.
[7] Bourc'his, D., Xu, G.L., Lin, C.S., Bollman, B. and Bestor, T.H. (2001) Dnmt3L and the establishment of maternal genomic imprints. Science 294, 2536–2539.
[8] Hata, K., Okano, M., Lei, H. and Li, E. (2002) Dnmt3L cooperates with the Dnmt3 family of de novo DNA methyltransferases to establish maternal imprints in mice. Development 129, 1983–1993.
[9] Kaneda, M., Okano, M., Hata, K., Sado, T., Tsujimoto, N., Li, E. and Sasaki, H. (2004) Essential role for de novo DNA methyltransferase Dnmt3a in paternal and maternal imprinting. Nature 429, 900–903.
[10] Thorvaldsen, J.L., Duran, K.L. and Bartolomei, M.S. (1998) Deletion of the H19 differentially methylated domain results in loss of imprinted expression of H19 and Igf2. Genes Dev. 12, 3693–3702.
[11] Bielinska, B., Blaydes, S.M., Buiting, K., Yang, T., Krajewska-Walasek, M., Horsthemke, B. and Brannan, C.I. (2000) De novo deletions of SNRPN exon 1 in early human and mouse embryos result in a paternal to maternal imprint switch. Nat. Genet. 25, 74–78.
[12] Wutz, A., Theussl, H.C., Dausman, J., Jaenisch, R., Barlow, D.P. and Wagner, E.F. (2001) Non-imprinted Igf2r expression decreases growth and rescues the Tme mutation in mice. Development 128, 1881–1887.
[13] Fitzpatrick, G.V., Soloway, P.D. and Higgins, M.J. (2002) Regional loss of imprinting and growth deficiency in mice with a targeted deletion of KvDMR1. Nat. Genet. 32, 426–431.
[14] Yoon, B.J., Herman, H., Sikora, A., Smith, L.T., Plass, C. and Soloway, P.D. (2002) Regulation of DNA methylation of Rasgrf1. Nat. Genet. 30, 92–96.
[15] Lin, S.P., Youngson, N., Takada, S., Seitz, H., Reik, W., Paulsen, M., Cavaille, J. and Ferguson-Smith, A.C. (2003) Asymmetric regulation of imprinting on the maternal and paternal chromosomes at the Dlk1-Gtl2 imprinted cluster on mouse chromosome 12. Nat. Genet. 35, 97–102.
[16] Williamson, C.M. et al. (2004) A cis-acting control region is required exclusively for the tissue-specific imprinting of Gnas. Nat. Genet. 36, 894–899.
[17] Liu, J., Chen, M., Deng, C., Bourc'his, D., Nealon, J.G., Erlichman, B., Bestor, T.H. and Weinstein, L.S. (2005) Identification of the control region for tissue-specific imprinting of the stimulatory G protein alpha-subunit. Proc. Natl. Acad. Sci. USA 102, 5513–5518.
[18] Williamson, C.M. et al. (2006) Identification of an imprinting control region affecting the expression of all transcripts in the Gnas cluster. Nat. Genet. 38, 350–355.
[19] Shiura, H. et al. (2009) Paternal deletion of Meg1/Grb10 DMR causes maternalization of the Meg1/Grb10 cluster in mouse proximal chromosome 11 leading to severe pre- and postnatal growth retardation. Hum. Mol. Genet. 18, 1424–1438.
[20] Babak, T., Deveale, B., Armour, C., Raymond, C., Cleary, M.A., van der Kooy, D., Johnson, J.M. and Lim, L.P. (2008) Global survey of genomic imprinting by transcriptome sequencing. Curr. Biol. 18, 1735–1741.
[21] Kobayashi, H. et al. (2009) Identification of the mouse paternally expressed imprinted gene Zdbf2 on chromosome 1 and its imprinted human homolog ZDBF2 on chromosome 2. Genomics 93, 461–472.
[22] Hiura, H. et al. (2010) A tripartite paternally methylated region within the Gpr1-Zdbf2 imprinted domain on mouse chromosome 1 identified by meDIP-on-chip. Nucleic Acids Res. 38, 4929–4945.
[23] Kobayashi, H. et al. (2012) Contribution of intragenic DNA methylation in mouse gametic DNA methylomes to establish oocyte-specific heritable marks. PLoS Genet. 8, e1002440.
[24] Sleutels, F., Zwart, R. and Barlow, D.P. (2002) The non-coding Air RNA is required for silencing autosomal imprinted genes. Nature 415, 810–813.
[25] Mancini-Dinardo, D., Steele, S.J., Levorse, J.M., Ingram, R.S. and Tilghman, S.M. (2006) Elongation of the Kcnq1ot1 transcript is required for genomic imprinting of neighboring genes. Genes Dev. 20, 1268–1282.
[26] Williamson, C.M. et al. (2011) Uncoupling antisense-mediated silencing and DNA methylation in the imprinted Gnas cluster. PLoS Genet. 7, e1001347.
[27] Chotalia, M. et al. (2009) Transcription is required for establishment of germline methylation marks at imprinted genes. Genes Dev. 23, 105–117.
[28] Arnaud, P., Hata, K., Kaneda, M., Li, E., Sasaki, H., Feil, R. and Kelsey, G. (2006) Stochastic imprinting in the progeny of Dnmt3L−/− females. Hum. Mol. Genet. 15, 589–598.
[29] Kumaki, Y., Oda, M. and Okano, M. (2008) QUMA: quantification tool for methylation analysis. Nucleic Acids Res. 36, W170–W175.
[30] Guttman, M. et al. (2010) Ab initio reconstruction of cell type-specific transcriptomes in mouse reveals the conserved multi-exonic structure of lincRNAs. Nat. Biotechnol. 28, 503–510.
[31] Ohhata, T., Senner, C.E., Hemberger, M. and Wutz, A. (2011) Lineage-specific function of the noncoding Tsix RNA for Xist repression and Xi reactivation in mice. Genes Dev. 25, 1702–1715.
[32] Ng, K., Pullirsch, D., Leeb, M. and Wutz, A. (2007) Xist and the order of silencing. EMBO Rep. 8, 34–39.
[33] Rinn, J.L. et al. (2007) Functional demarcation of active and silent chromatin domains in human HOX loci by noncoding RNAs. Cell 129, 1311–1323.
[34] Henckel, A., Chebli, K., Kota, S.K., Arnaud, P. and Feil, R. (2012) Transcription and histone methylation changes correlate with imprint acquisition in male germ cells. EMBO J. 31, 606–615.
[35] Zhang, Y. et al. (2010) Chromatin methylation activity of Dnmt3a and Dnmt3a/3L is guided by interaction of the ADD domain with the histone H3 tail. Nucleic Acids Res. 38, 4246–4253.
[36] Dhayalan, A., Rajavelu, A., Rathert, P., Tamas, R., Jurkowska, R.Z., Ragozin, S. and Jeltsch, A. (2010) The Dnmt3a PWWP domain reads histone 3 lysine 36 trimethylation and guides DNA methylation. J. Biol. Chem. 285, 26114–26120.

RESEARCH PAPER

Epigenetics 7:2, 173-182; February 2012; © 2012 Landes Bioscience

Trophoblast-specific DNA methylation occurs after the segregation of the trophectoderm and inner cell mass in the mouse periimplantation embryo

Momo O. Nakanishi,[1] Koji Hayakawa,[1] Kazuhiko Nakabayashi,[2] Kenichiro Hata,[2] Kunio Shiota[1] and Satoshi Tanaka[1,*]

[1]Laboratory of Cellular Biochemistry; Department of Animal Resource Sciences/Veterinary Medical Sciences; The University of Tokyo; Tokyo, Japan;
[2]Department of Maternal-Fetal Biology; National Research Institute for Child Health and Development; Tokyo, Japan

Key words: DNA methylation, trophoblast, blastocyst, trophectoderm, placenta

Abbreviations: E, embryonic day; ES, embryonic stem; EPC, ectoplacental cone; Epi, epiblast; ExE, extraembryonic ectoderm; FBS, fetal bovine serum; ICM, inner cell mass; MSRE-qPCR, methylation-sensitive restriction enzyme-quantitative PCR; PBS, phosphate buffered saline; PCR, polymerase chain reaction; PVP, polyvinylpyrrolidone; RLGS, restriction landmark genomic scanning; T-DMRs, tissue-dependent and differentially methylated region; TE, trophectoderm; TS, trophoblast stem

The first cell differentiation in the mammalian development separates the trophoblast and embryonic cell lineages, resulting in the formation of the trophectoderm (TE) and inner cell mass (ICM) in blastocysts. Although a lower level of global DNA methylation in the genome of the TE compared with ICM has been suggested, the dynamics of the DNA methylation profile during TE/ICM differentiation has not been elucidated. To address this issue, first we identified tissue-dependent and differentially methylated regions (T-DMRs) between trophoblast stem (TS) and embryonic stem (ES) cells. Most of these TS-ES T-DMRs were also methylated differentially between trophoblast and embryonic tissues of embryonic day (E) 6.5 mouse embryos. Furthermore, we found that the human genomic regions homologous to mouse TS-ES T-DMRs were methylated differentially between human placental tissues and ES cells. Collectively, we defined them as cell-lineage-based T-DMRs between trophoblast and embryonic cell lineages (T-E T-DMRs). Then, we examined TE and ICM cells isolated from mouse E3.5 blastocysts. Interestingly, all T-DMRs examined, including the *Elf5*, *Pou5f1* and *Nanog* loci, were in the nearly unmethylated status in both TE and ICM and exhibited no differences. The present results suggest that the establishment of DNA methylation profiles specific to each cell lineage follows the first morphological specification. Together with previous reports on asymmetry of histone modifications between TE and ICM, the results of the current study imply that histone modifications function as landmarks for setting up cell-lineage-specific differential DNA methylation profiles.

Introduction

DNA methylation is one of the epigenetic modifications in mammals and affects the functional state of the genome. In the developmental process, cells arising from the single cell, i.e., fertilized zygotes, give rise to various types of cells via epigenetic drive, and cell differentiation is closely linked to the renovation of the epigenome. The mammalian genome contains tissue-dependent and differentially methylated regions (T-DMRs) that exhibit cell-type-specific DNA methylation levels.[1,2] Thus, the sum of DNA methylation status of T-DMRs is equivalent to cell-type-specific DNA methylation profiles,[3] i.e., cell differentiation is accompanied by the construction of new DNA methylation profiles.

The first cell differentiation in mammalian development segregates the trophoblast from the embryonic cell lineages. In mice, these two cell lineages are specified by embryonic day 3.5 (E3.5), which results in the formation of the trophectoderm (TE) and inner cell mass (ICM) of blastocysts. The TE gives rise exclusively to extraembryonic tissues, such as the placenta,[4] whereas the ICM gives rise to the embryo proper, germ cells and some extraembryonic membranes. As each cell type has its own distinctive DNA methylation profile, it is assumed that cells of the TE and ICM also have their unique DNA methylation profiles, which suggests the presence of T-DMRs between the TE and ICM (TE-ICM T-DMRs).

Differences in DNA methylation levels between extraembryonic and embryonic tissues were reported in the 1980s in studies using postimplantation-stage embryos. Hypomethylation in extraembryonic tissues compared with embryonic tissues was first found in the rabbit;[5] subsequently, it was confirmed in the

*Correspondence to: Satoshi Tanaka; Email: asatoshi@mail.ecc.u-tokyo.ac.jp
Submitted: 10/21/11; Revised: 12/02/11; Accepted: 12/06/11
http://dx.doi.org/10.4161/epi.7.2.18962

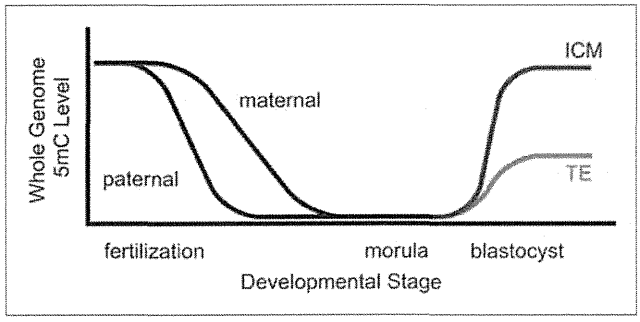

Figure 1. Schematic diagram of the dynamic change in the 5-methylcytosine levels of the whole genome in mouse preimplantation embryos. The x-axis (time) and the y-axis (relative 5-mC levels of genomic DNA) are not to scale. Modified from Dean et al.[10]

mouse at the level of not only total DNA, but also at repetitive elements and some unique genes.[6-8] However, the process of the establishment of such differences in DNA methylation remained unclear because it was technically difficult to analyze the DNA methylation state in trophoblast and embryonic tissues separately using preimplantation embryos. Currently, this issue is explained by differences in the extent of de novo methylation in the preimplantation stage, which was shown in a recent report that examined changes in DNA methylation levels via immunostaining of mouse embryos at sequential stages using an anti-5-methylcytosine (5-mC) antibody.[9] After fertilization, there is a drastic decrease in the content of 5-mC in genomic DNA.[10-12] Thus, 5-mC is barely detected at the morula stage, which is followed by de novo methylation that results in detectable levels of 5-mC in E3.5 blastocysts. In the blastocyst, higher levels of the methylated signal were observed in the ICM compared with the TE.[9] Based on these findings, the wave of DNA methylation dynamics shown in **Figure 1** is currently well accepted.[10] It should be mentioned, however, that this wave represents the global change in the methylation level of the whole genome. In fact, some individual loci and repetitive elements, in addition to imprinted gene loci, do not follow this wave.[13-16] In addition, recent reports suggest that the conversion of 5-mC to 5-hydroxymethyl-cytosine accounts for rapid reduction of 5-mC in male pronuclei in zygotes.[17,18]

Cultured stem cell lines have been derived from the TE and ICM: trophoblast stem (TS) cells[19] and embryonic stem (ES) cells,[20,21] respectively. Because their developmental potentials correspond well with their tissues of origin, these cells have been used as in vitro models. It was reported that some lineage-specific genes are regulated via DNA methylation in TS and ES cells. ELF5 is expressed specifically in extraembryonic tissues in mouse embryos and is required for the maintenance of TS cells.[22] In ES cells, ELF5 expression is repressed by the highly methylated status of the upstream region, preventing a trophoblastic cell fate. In contrast, the *Elf5* locus is not methylated in TS cells, which express ELF5.[23] Conversely, we have reported that the pluripotency-related genes *Pou5f1* and *Nanog*[24-27] exhibit an expression pattern that is opposite to that of *Elf5*.[28,29] Namely, the *Pou5f1* and *Nanog* loci contain T-DMRs that are hypermethylated in TS cells and hypomethylated in ES cells. However, whether such T-DMRs between TS and ES cells (TS-ES T-DMRs) represent faithfully TE-ICM T-DMRs has not been elucidated. It was reported previously that the *Pou5f1* and *Nanog* loci are scarcely methylated in E3.5 embryos,[30,31] but TE and ICM were not analyzed separately in these reports; thus, whether these loci are T-DMRs remains unclear.

DNA methylation profiles reflect the multilayered regulation of tissue-specific gene function.[32,33] In addition, the analysis of the methylation profile of 18 different tissues and cells revealed that DNA methylation profiles reflect developmental similarity and cellular phenotypes.[34] Thus, TS-ES T-DMRs potentially represent the prime difference between trophoblast and embryonic cell lineages, and are considered as good candidates for TE-ICM T-DMRs. In this study, we elucidated the DNA methylation status of TS-ES T-DMRs in trophoblast and embryonic lineages in the mouse embryo to determine definitively whether T-DMRs defined between TS cells and ES cells are established as TE-ICM T-DMRs in the developmental process.

Results

Identification of novel TS-ES T-DMRs. In our effort to identify T-DMRs in the mouse genome, we sampled more than 200 *NotI* recognition sites as potentially informative loci and examined their DNA methylation status using real-time quantitative methylation-sensitive restriction enzyme PCR (MSRE-qPCR) in various cells and tissues.[34] Through this effort, we also identified several *NotI* sites as potential TS-ES T-DMRs showing differential methylation levels between TS and ES cells (data not shown). Some of these sites were used in our previous reports to verify the epigenetic integrity of TS and ES cells derived from somatic cell nuclear-transferred embryos.[35,36]

In this study, we selected 14 potential TS-ES T-DMRs from the MSRE-qPCR data set based on the criteria mentioned in the Materials and Methods. All of these loci were hypermethylated in TS cells and hypomethylated in ES cells. We performed bisulfite sequencing analysis of the regions around these *NotI* sites to elucidate the regional DNA methylation status. Among them, seven regions (*Ff46*, *Bd22*, *Ef40*, *Hd20*, *Eb41*, *Ff36* and *Hf01*; Group A) exhibited a markedly hypermethylated status in TS cells (at least 40% higher in TS than in ES cells); thus, these were confirmed as definite TS-ES T-DMRs (**Fig. 2 and Table 1**). Five regions (*Gc06*, *Eg01*, *Ef30*, *Ca37* and *Gb20*; Group B) also showed higher DNA methylation status in TS vs. ES cells, but with a moderate difference (30–40%). The other two regions (*Ec23* and *He06*) showed only a modest difference (<15%; Group C). Thus, we successfully identified TS-ES T-DMRs that are good candidates for T-DMRs between trophoblast and embryonic cell lineages in vivo.

DNA methylation status of TS-ES T-DMRs in the extraembryonic ectoderm (ExE) and epiblast (Epi) of E6.5 embryos and in E14.5 placenta. Having identified TS-ES T-DMRs, we then analyzed their DNA methylation status in the ExE and Epi of E6.5 postimplantation embryos to ascertain whether they were methylated differentially in vivo. The ExE and Epi originate from the TE and ICM, respectively. TS cell lines can also be derived

from the ExE of E6.5 embryos;[19,37] thus, it is implied that stem cells of the trophoblast lineage are maintained in E6.5 ExE. At the *Ddah2* gene locus, the epigenetic properties of the ExE were reflected in that of TS cells.[38]

Among the TS-ES T-DMRs identified above, all seven loci from Group A and four loci (*Gc06*, *Eg01*, *Ca37* and *Gb20*) from Group B showing <5% methylation in ES cells were selected for analysis. The ExE and Epi from a single embryo were used for single-locus analysis. Bisulfite sequencing analysis revealed three types of methylation pattern. First, eight loci (*Ff46*, *Hd20*, *Eb41*, *Ff36*, *Hf01*, *Gc06*, *Eg01* and *Ca37*) were hypermethylated in ExE and hypomethylated in Epi ($p < 0.01$), as expected from the methylation trend observed in TS and ES cells (**Fig. 3A and Table S1**). Second, *Ef40* was also methylated differentially between ExE and Epi, but the methylation trend was opposite to that observed in cells in vitro (**Fig. S1 and Table S1**). Finally, there was very little methylation difference at the *Gb20* and *Bd22* loci (<8%) between ExE and Epi (**Fig. S1 and Table S1**).

We also examined the methylation status of the three TS-ES T-DMRs reported previously (*Elf5*, *Pou5f1* and *Nanog*),[23,28,29] and observed that all three loci were hypermethylated or hypomethylated in ExE and Epi in the same manner as that observed in TS cells and ES cells (**Fig. 3B and Table S1**); namely, the *Elf5* locus was hypomethylated in ExE and hypermethylated in Epi, and converse findings were obtained at the *Pou5f1* and *Nanog* loci. Although the tendency of the methylation pattern was consistent throughout every experiment, the extent of methylation varied among embryos at some loci. Most conspicuously, between two embryos analyzed, the extent of methylation of *Pou5f1* in ExE was lower in one embryo than in the other. This may indicate that differential methylation is still in the process of being established at E6.5; thus, some embryos are a little more advanced than others. Nevertheless, these loci were confirmed as T-DMRs between trophoblast and embryonic lineages in vivo at E6.5 (ExE-Epi T-DMRs), as reflected in TS and ES cells.

Collectively, most of the TS-ES T-DMRs were ExE-Epi T-DMRs and can be defined as trophoblast-embryonic T-DMRs (T-E T-DMRs) in vivo. No common features were found among these T-E T-DMRs regarding chromosomal location, relative position to the nearest genes and CpG islands (**Fig. S2**).

We also checked whether T-E T-DMRs were hypermethylated in the placenta. Bisulfite sequencing of the eight T-E T-DMR loci was performed in mouse E14.5 placenta and showed that the T-E T-DMRs were also hypermethylated in the placenta, almost equally to that observed for E6.5 ExE, with only one exception: *Hd20* was scarcely methylated (**Fig. S3**). The methylation rates in placenta were lower than those observed in TS cells, which is consistent with our previous analysis using the MSRE-qPCR method (unpublished data and ref. 34). In the present study, ExE also showed a lower extent of hypermethylation compared with that of TS cells. Previously, it was shown that the methylation extent at the *Pou5f1* and *Ddah2* loci in the placenta and ExE was lower than that observed in TS cells, respectively.[28,38] This may reflect the heterogeneity of in vivo tissue samples.

DNA methylation status of T-E T-DMRs in human placenta and ES cells. To investigate whether the cell-lineage-based differential DNA methylation pattern at T-E T-DMR loci is also present in other mammalian species, we analyzed the DNA methylation status in human samples. Because it is ethically difficult to use human early-stage embryos, we used later-stage placental tissues.

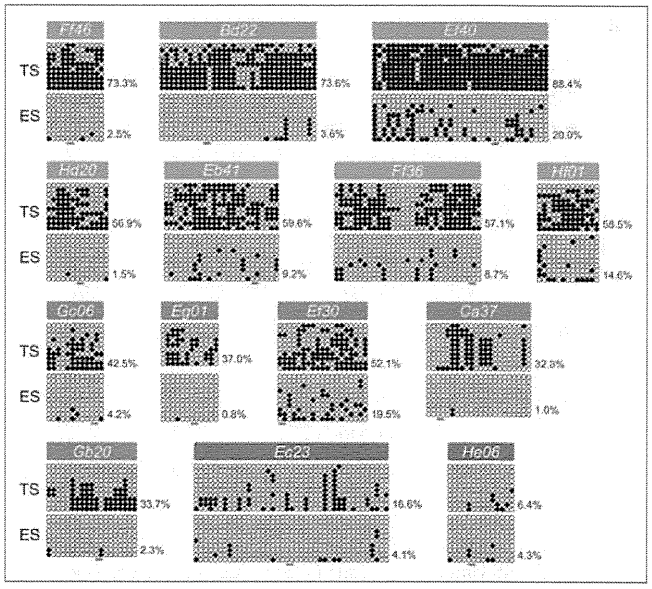

Figure 2. DNA methylation status of the TS-ES T-DMRs around the *NotI* site in TS and ES cells. The DNA methylation status of potential TS-ES T-DMRs around the *NotI* site were determined via bisulfite sequencing. Open and filled circles represent unmethylated and methylated cytosines, respectively. X, not read by sequence analysis. Overall methylation percentage (the number of methylated CpGs per number of total CpGs) is shown to the right side of each part. The red bars under each part indicate CpGs at the *NotI* site. For *Hf01*, the region upstream of the *NotI* site was analyzed in this study. TS-ES T-DMRs were classified into three groups according to the extent of differences between TS and ES cells: seven loci as Group A (shown in the pink box); five loci as Group B (shown in the purple box); and two loci as Group C (shown in the gray box).

The sequences of the eight loci confirmed as T-E T-DMRs in mice (*Ff46*, *Hd20*, *Eb41*, *Ff36*, *Hf01*, *Gc06*, *Eg01* and *Ca37*) are conserved in the human genome (**Table S2 and Fig. S4**). We performed bisulfite sequencing analysis of these homologous regions using human cells and tissues. Placental villus samples from gestational stages under 14 weeks (u14wks) of pregnancy and term placenta, and human ES (hES) cells were used as trophoblastic and embryonic samples, respectively. The bisulfite PCR amplicons were designed to cover the conserved genomic regions (**Table S2**). Consequently, all regions examined were hypermethylated in u14wks and/or term placental tissues and hypomethylated in ES cells ($p < 0.01$) (**Fig. 4**). These results demonstrate that trophoblast cell-lineage-specific hypermethylation is conserved between mice and humans at these T-E T-DMRs.

DNA methylation status of T-E T-DMRs in E3.5 blastocysts. As shown above, cell-lineage-based differences between trophoblast and embryonic cell lineages regarding DNA methylation exist at T-E T-DMR loci in E6.5 mouse embryo. To assess whether this difference exists in E3.5 blastocysts, we collected

Table 1. DNA methylation rate of TS-ES T-DMRs in TS and ES cells

Locus	TS*	(%)	ES*	(%)	TS-ES (%)	p value**	Group
Ff46	88/120	73.3	3/120	2.5	70.8	2.2×10^{-5}	A
Bd22	242/329	73.6	12/330	3.6	70.0	1.1×10^{-5}	A
Ef40	327/370	88.4	74/370	20.0	68.4	1.1×10^{-5}	A
Hd20	74/130	56.9	2/130	1.5	55.4	1.7×10^{-4}	A
Eb41	143/240	59.6	22/240	9.2	50.4	1.1×10^{-5}	A
Ff36	177/310	57.1	27/310	8.7	48.4	1.1×10^{-5}	A
Hf01	76/130	58.5	19/130	14.6	43.9	2.3×10^{-3}	A
Gc06	51/120	42.5	5/120	4.2	38.3	9.3×10^{-4}	A
Eg01	40/108	37.0	1/120	0.8	36.2	2.3×10^{-4}	A
Ef30	99/190	52.1	37/190	19.5	32.6	1.0×10^{-3}	B
Ca37	71/220	32.3	2/198	1.0	31.3	2.2×10^{-5}	B
Gb20	64/190	33.7	4/171	2.3	31.3	1.5×10^{-2}	B
Ec23	68/410	16.6	17/410	4.1	12.4	4.8×10^{-3}	C
He06	9/140	6.4	6/140	4.3	2.1	7.4×10^{-1}	C

*Number of methylated CpGs/total number of CpGs analyzed using the bisulfite sequencing illustrated in **Figure 2**. **p values were calculated using the nonparametric two-tailed Mann-Whitney test.

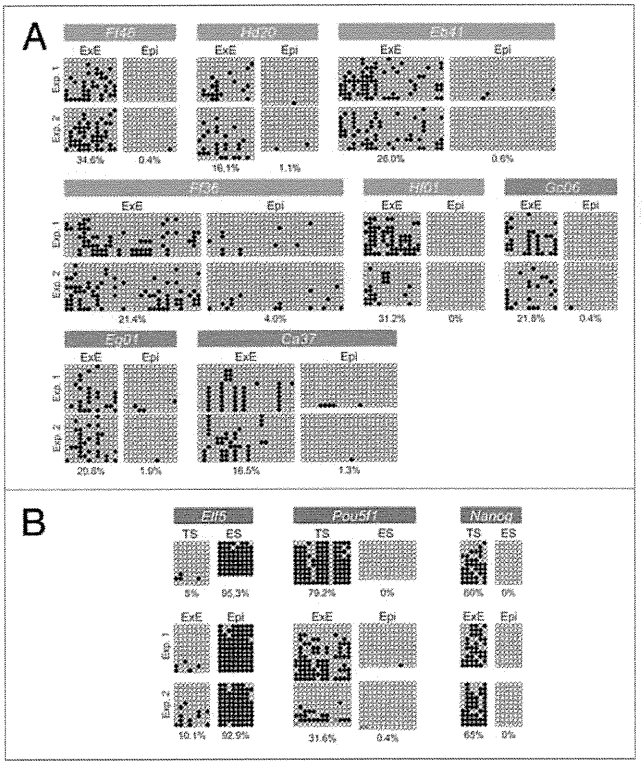

Figure 3. DNA methylation status of TS-ES T-DMRs in the ExE and Epi. (A) DNA methylation status of eight TS-ES T-DMRs around *NotI* sites in the ExE and Epi, as determined using bisulfite sequencing. Samples for experiments 1 (Exp. 1) and 2 (Exp. 2) were collected independently. The color of boxes indicates the group defined by the methylation status of TS and ES cells (see **Fig. 2** and **Table 1**). (B) DNA methylation status of *Elf5*, *Pou5f1* and *Nanog* in TS cells, ES cells, ExE and Epi, as determined using bisulfite sequencing. Open and filled circles represent unmethylated and methylated cytosines, respectively. Overall methylation percentage (the number of methylated CpGs per number of total CpGs) is shown under each part.

E3.5 blastocysts and isolated TE and ICM cells enzymatically, to analyze their DNA methylation status separately.

Because the number of TE and ICM cells available after completion of this separating method was very limited, we assessed the fidelity of the bisulfite sequencing analysis using as few as 100 cells before the analysis of the TE and ICM cells. We designed two experiments with ~100 cells in which the methylation status would be ~50% theoretically. First, we examined the DNA methylation status of the *H19* locus using two E3.5 blastocysts. *H19*, an imprinted locus, is methylated only at the paternal allele in E3.5 embryos.[39] As shown in **Figure S5A**, both methylated and unmethylated clones emerged, although the methylation rate was not exactly 50%. Next, DNA methylation status was analyzed at the *Elf5* and *Pou5f1* using a 1:1 mixture of TS and ES cells. Trypsinized cells were counted and collected under a dissecting microscope, and 50 cells of each type were combined to obtain 100 cells in total per analysis of each locus. The T-DMR at the *Elf5* locus was methylated at ~100% in ES cells and at ~0% in TS cells, whereas that at the *Pou5f1* locus exhibited the opposite methylation pattern (reviewed in refs. 23 and 28 and this study). Theoretically, the 1:1 cell mixture should exhibit ~50% methylation at these two loci. In our study, although the methylation level was not exactly 50%, methylated and unmethylated DNA strands were detected at both loci and the methylation rate was around 50% (**Fig. S5B**). Therefore, we concluded that the method adopted here provides the methylation status in samples of ~100 cells, although its accuracy did not reach the predicted methylation value exactly.

The results of the bisulfite sequencing analysis using TE and ICM cells demonstrated that the three T-E T-DMRs *Elf5*, *Pou5f1* and *Hf01* were remarkably hypomethylated in both the TE and ICM, and that there was no difference in DNA methylation rate between the TE and ICM ($p > 0.05$) (**Fig. 5A**). The T-DMRs at the *Elf5* and *Pou5f1* loci were almost completely unmethylated, which is consistent with the results of a previous study based

on whole blastocysts.[30,40] *Hf01* also showed a hypomethylated status; however, there were more methylated CpGs at this locus than at *Elf5* and *Pou5f1* in both the TE and ICM. To summarize, all three T-E T-DMRs were in a state of hypomethylation in both E3.5 TE and ICM.

Because the three T-E T-DMRs examined above appeared to be barely methylated and showed no apparent difference between the TE and ICM, we explored whether there was any DNA methylation at other T-E T-DMRs in E3.5 blastocysts. Thus, we evaluated the DNA methylation status of the other eight T-E T-DMRs (*Ff46*, *Hd20*, *Eb41*, *Ff36*, *Gc06*, *Eg01*, *Ca37* and *Nanog*) in whole blastocysts. As shown in **Figure 5B**, we found that these loci exhibited little or no methylation in E3.5 blastocysts, which led us to conclude that all T-E T-DMRs examined here were almost totally hypomethylated in E3.5 blastocysts, whether in the TE or ICM.

DNA methylation status of T-E T-DMRs in E4.5 and diapause blastocysts. Having demonstrated that all T-E T-DMRs were scarcely methylated in blastocysts at E3.5, we then examined the methylation status of T-E T-DMRs in E4.5 blastocysts flushed out from uteri. The following four loci were selected for examination: *Ff46*, *Eb41* (especially highly methylated in E6.5 ExE and in E14.5 placenta), *Nanog* (the most methylated locus in E6.5 ExE) and *Elf5* (the only locus that was hypermethylated in the embryonic cell lineage examined in this study). We observed that all four loci examined were hypomethylated in E4.5 blastocysts, to the same extent as that observed at E3.5 (**Fig. 6A**).

We also examined the DNA methylation status of the four loci in diapause blastocysts obtained via experimentally induced delayed implantation. A slight increase in methylation rate was observed in diapause blastocysts compared with E4.5 blastocysts; however, this difference was not significant, with the exception of the results obtained for *Elf5* ($p < 0.01$) (**Fig. 6B**).

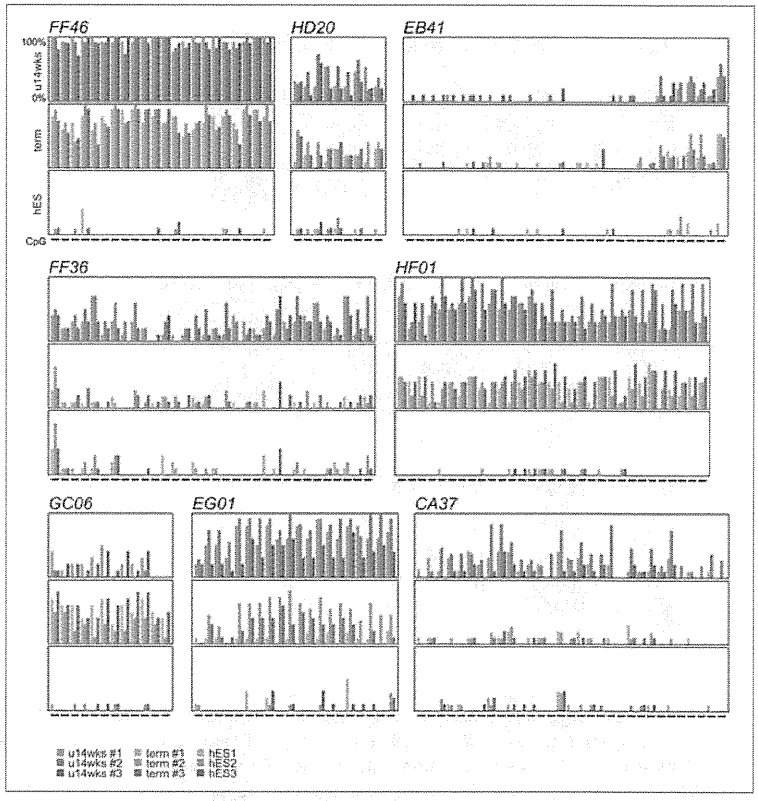

Figure 4. DNA methylation status of T-E T-DMRs in human placenta and ES cells. Graphic representation of the DNA methylation level at human genomic regions homologous to mouse T-E T-DMRs in human placental tissue from under 14 weeks of gestation (u14wks), from term pregnancy (term), and from human ES cells (hES). Three independent samples or cell lines were examined for each tissue/cell type. CpG sites are indicated by short horizontal bars at the bottom of each part. The percentage ratio of methylated cytosines at each CpG site, which was determined from the data of clone-based bisulfite sequencing, is indicated by vertical columns, with the height of each column representing the degree of methylation.

Discussion

Here, we identified T-E T-DMRs that were methylated differentially between trophoblast and embryonic cell lineages both in vitro and in vivo. Regarding the correspondence between the DNA methylation patterns in vitro and in vivo, this epigenetic feature observed at our T-E T-DMRs is likely an inherent property of each cell lineage. Using these T-E T-DMRs, we traced and delineated the trophoblast/embryonic cell lineage differentiation from the viewpoint of the DNA methylation profile and observed that the T-E T-DMRs *Elf5*, *Pou5f1* and *Hf01* were scarcely methylated in both the TE and ICM. The nearly unmethylated status observed in whole blastocysts was also present in all other T-E T-DMR loci. Collectively, all T-E T-DMR loci examined were almost unmethylated in E3.5 mouse blastocysts. This is of interest because the TE and ICM are specified distinctly to each cell lineage; thus, each of these structures was expected to exhibit a different methylation pattern at the T-E T-DMRs.

It is known that the expression of *Elf5*, *Pou5f1* and *Nanog* is regulated via DNA methylation in TS and ES cells.[23,28,29] However, in this study, these genes showed little methylation both in TE and ICM, which exhibit a differential expression pattern.[22,41] This result indicates that the transcription of these genes is not regulated in a DNA-methylation-dependent manner in the blastocyst. In a recent study, an *Elf5* transgene lacking the differentially methylated region did not show ectopic expression in blastocysts.[42] Moreover, nuclear-transferred embryos with no functional DNA methyltransferase can reach the blastocyst stage.[43] Based on these observations, DNA methylation is considered dispensable in regulating the expression of the factors necessary for TE/ICM differentiation.

The present study provides an additional epigenetic insight into trophoblast/embryonic cell differentiation. We demonstrated clearly that the trophoblast and embryonic cell-lineage-specific DNA methylation patterns of T-E T-DMRs are set up by E6.5,

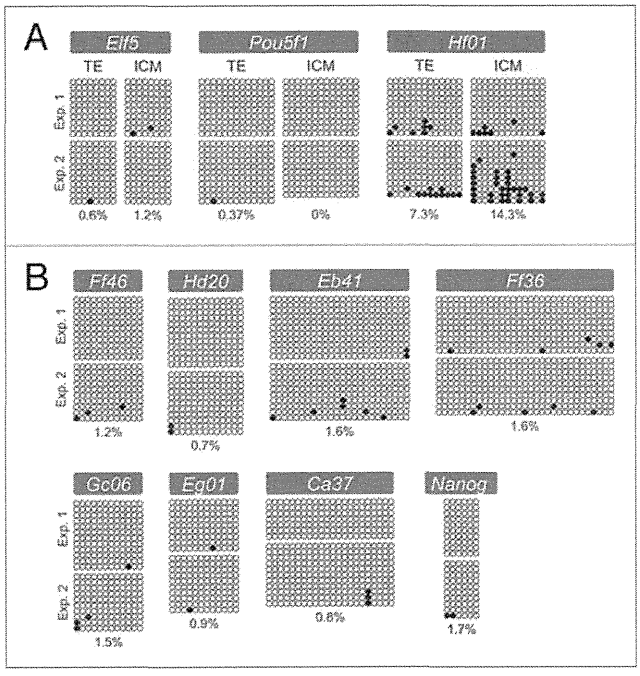

Figure 5. DNA methylation status of T-E T-DMRs in E3.5 blastocysts. (A) DNA methylation status of *Elf5*, *Pou5f1* and *Hf01* in the TE and ICM of E3.5 blastocysts. (B) DNA methylation status of the T-E T-DMRs *Ff46*, *Hd20*, *Eb41*, *Ff36*, *Gc06*, *Eg01*, *Ca37* and *Nanog* in E3.5 blastocysts, as determined using bisulfite sequencing. Open and filled circles represent unmethylated and methylated cytosines, respectively. Overall methylation percentage (the number of methylated CpGs per number of total CpGs) is shown under each part.

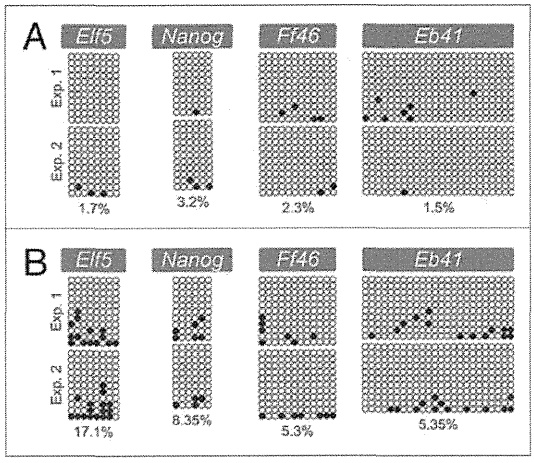

Figure 6. DNA methylation status of T-E T-DMRs in E4.5 and diapause blastocysts. DNA methylation status of selected T-E T-DMRs (*Elf5*, *Nanog*, *Ff46* and *Eb41*) in E4.5 (A) and diapause (B) blastocysts. Open and filled circles represent unmethylated and methylated cytosines, respectively. Overall methylation percentage (the number of methylated CpGs per number of total CpGs) is shown under each part.

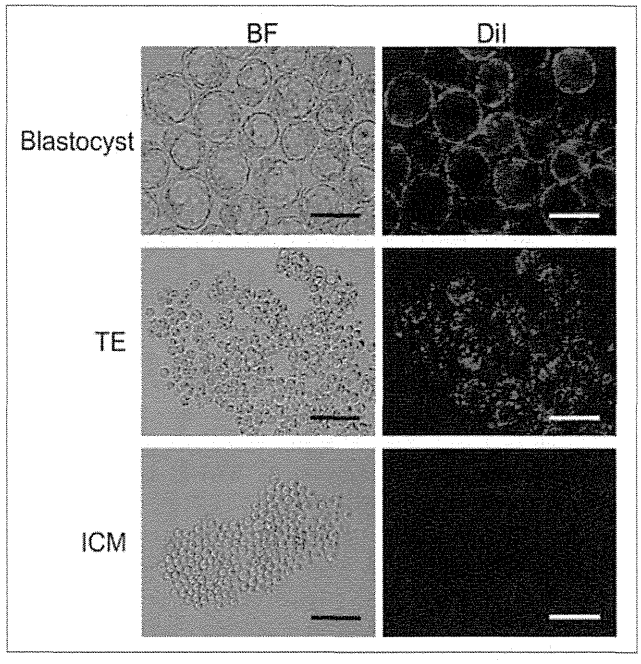

Figure 7. Separation of TE and ICM cells. Top, intact blastocysts stained with DiI at the outer surface. Middle, cells with DiI fluorescence (TE). Bottom, cells without DiI fluorescence (ICM). Scale bars, 100 μm. BF, bright field.

but not at E3.5. The comparison of E4.5 and diapause blastocysts revealed the presence of a slight, yet significant, increase in the DNA methylation level at the *Elf5* locus in diapause blastocysts. It is possible that de novo methylation gradually progresses in the ICM during the few days of diapause. Alternatively, gradual de novo methylation may have started in the advanced, already implanted embryos at E4.5, which were not recovered by uterine flushing. Nevertheless, our results demonstrate that de novo methylation of T-E T-DMRs occurs after TE/ICM specification.

Our observations suggest that factors other than DNA methylation lead TE/ICM differentiation. In addition to the balance of key transcription factors and apical/basal cell polarity, epigenetic modification on histone tails is another potential differentiation-leading factor. The histone modification status of some genes in the TE and ICM was analyzed previously in reference 44. In the ICM, the promoter regions of *Pou5f1* and *Nanog* are enriched in H4K16 acetylation, which is a permissive modification, whereas repressive modification of H3K9 dimethylation is depleted. In contrast, the converse is true in the TE. These modification patterns correspond to the transcriptional states of these genes. Furthermore, at an earlier stage after the first cleavage, it is suggested that histone modification asymmetry in two blastomeres functions as an epigenetic marker for cell allocation in extraembryonic or embryonic lineages.[45] Together with our present results, these data imply that preceding histone modifications may be landmarks for the establishment of trophoblast-specific DNA methylation profiles during trophoblast and embryonic cell-lineage segregation, because interactions between

histone modification and DNA methylation have been observed in many studies,[46,47] although whether this is true remains an open question.

Our results also showed that TS and ES cells are distinct from their corresponding tissues of origin in blastocysts. Based on transcriptome analysis, some reports showed that the global gene expression patterns of ES cells and the ICM are significantly different.[48,49] The present study confirmed this notion epigenetically in TS cells and in the TE from the viewpoint of DNA methylation. There are two possible explanations for this: one is that the culture conditions and microenvironment enhanced de novo DNA methylation; the other is that there is a very small subset of cells in blastocysts with a highly methylated status that are selected to survive and expand in culture. Drastic changes during the cell-line derivation process were reported recently in studies of other aspects of the epigenome. One heterochromatic histone modification is acquired during culture for ES cell derivation, and culture conditions have some effect on this phenomenon.[50] The stem cell derivation process from blastocysts is accompanied by revisions of the epigenome.

Our observations suggest that, when TS cells are derived from E3.5 TE, a TS cell-specific DNA methylation profile is acquired during the cell culture process. In our previous study, TS cells derived from blastocysts via nuclear transfer (ntTS cells) exhibited a DNA methylation status that was very similar to that of TS cells derived from normally fertilized blastocysts,[36] although an aberrant methylation status has been reported for nuclear-transferred preimplantation embryos.[51,52] The present results raise a hypothesis to explain this observation: the DNA methylation profile is processed as TS cell-specific during cell-line derivation, even if somatic cell-specific DNA methylation marks remain in the TE of nuclear-transferred blastocysts.

Although TS cells can be derived from both types of tissue, TS cells are distinct from the TE and are rather similar to the ExE, from the viewpoint of the DNA methylation status of T-E T-DMRs. Previously, it was reported that TS cell lines can be derived from E6.5 ExE, but not from E3.5 TE in MAP3K4 (MEKK4)-deficient mice,[53] suggesting a different capacity to generate TS cells between MAP3K4-deficient TE and ExE. This phenotype possibly involves differences in epigenetic status between the TE and ExE.

In our MSRE-qPCR screening for TS-ES T-DMRs, we did not find T-DMRs that are hypermethylated specifically in ES cells. The seeming inconsistency between the present study and previous reports describing a hypomethylated genome in trophoblast cells[5-8] may be explained by the fact that we focused on CpGs of *NotI* sites, in contrast with the *HpaII* sites used in other reports. *NotI* and *HpaII* have a different tendency regarding the distribution of their recognition sites in the genome;[54] thus, the TS-ES T-DMRs tended to be located in CpG-rich portions of the genome (**Table S3**), where *NotI* sites are preferentially located. It has been suggested that 5-mC is converted to thymine (T) via spontaneous deamination.[55] Due to 5-mC-to-T conversion, CpG content might have gradually decreased over generations at genomic regions methylated in the epiblast that give rise to germ cells, which enriches the regions methylated in extraembryonic tissues among CpG-rich portions. This may underlie the unique epigenetic profile of trophoblast cells.

The eight T-E T-DMRs identified here were hypermethylated in trophoblast cells. Again, this is in contrast with the conventional understanding that global DNA methylation levels in extraembryonic tissues are lower than those of embryonic tissues. Previous reports indicated the hypomethylated status of placenta and extraembryonic tissues,[7,56] as was the case for TS cells (**Fig. S6 and Table S4**). Therefore, the significance of DNA methylation in trophoblast tissues has been downplayed. However, this study showed clearly the presence of genomic regions that were hypermethylated specifically in a trophoblast cell lineage, independently from the bulk genomic DNA methylation levels. A genome-wide survey of the promoter methylome in TS and ES cells via immunoprecipitation analysis using an anti-5-mC antibody identified several promoters that are hypermethylated in TS cells, and hypomethylated in ES cells.[31] Moreover, a genome-wide DNA methylation analysis using a methylation-sensitive restriction enzyme, restriction landmark genomic scanning (RLGS), revealed that methylation and demethylation occur to change the DNA methylation profile during the differentiation of rat trophoblastic cell lines.[57] In mouse embryos and TS cells, the DNA methylation status of the *Ddah2* gene in the trophoblast changes during the progression of the differentiation process.[38] As indicated by these findings, the establishment and modification of DNA methylation profiles clearly constitute the identity of trophoblast cells.

We found that the regions in the human genome that are homologous to mouse T-E T-DMRs are also hypermethylated in human placental tissues. A previous study of DNA methylation dynamics showed that the methylation level appeared higher in the TE than in the ICM in human blastocysts, as assessed using immunostaining;[58] this is in contrast with observations performed using mouse blastocysts.[9] Despite the presence of such differences between species, we identified genomic regions that were hypermethylated in trophoblastic tissues/cells and hypomethylated in embryonic tissues/cells, both in mouse and human samples. The fact that the epigenetic marks specific to the trophoblastic cell lineage were conserved across species raises the possibility that these epigenetic marks are somewhat meaningful for trophoblast identity.

In conclusion, the trophoblast or embryonic cell-lineage-based DNA methylation profile is constructed during native development after the segregation of the TE and ICM and during stem cell derivation. The T-E T-DMRs identified here will be used as an epigenetic indicator to advance the understanding of cell differentiation between trophoblast and embryonic cell lineages.

Materials and Methods

Mice. C57BL/6N and C57BL/6J mice were purchased from Japan CLEA and Charles River Japan, respectively. Both strains gave equivalent results and the data in the present study are a sum of the results obtained in these two strains. Animals were maintained under a 12 h light cycle. The experiments were performed according to the guidelines for the care and use of laboratory

animals (Graduate School of Agriculture and Life Sciences, University of Tokyo).

Embryo collection and manipulation. Preimplantation embryos were obtained from naturally mated or superovulated mature female mice. Copulation was determined by the presence of a vaginal plug and E0 was assumed to be midnight. E3.5 and E4.5 blastocysts were collected according to the standard protocol.[59] Briefly, blastocysts were collected by flushing uteri. After the removal of the zona pellucida using acid Tyrode's solution, blastocysts were incubated in KSOM (ARK Resource) containing Vybrant CM-DiI (1:200 dilution; Invitrogen, V22888) for 15–20 min at 37°C and 5% CO_2. Labeled blastocysts were washed in 0.25% PVP/PBS(-) several times. To segregate TE from ICM cells, washed blastocysts were then incubated at room temperature in 1.25% pancreatin (Wako Pure Chemicals, 163-00142)/0.25% trypsin (Invitrogen)/ 1 mM EDTA/PBS(-). Five minutes after the start of the incubation, blastocysts were pipetted in enzyme solution through a fine glass pipette (~50 μm diameter) to dissociate blastomeres. The enzyme reaction was stopped with 10% FBS/PBS(-) before the enzyme treatment exceeded 10 min. Cells with and without DiI fluorescence were collected as TE and ICM cells, respectively, under a fluorescence microscope equipped with micromanipulators (Olympus) (**Fig. 7**).

Induction of delayed implantation was performed according to the standard protocol,[59] with a slight modification. Briefly, pregnant mice were ovariectomized in the morning of E3.5 and injected daily with progesterone (2 mg per mouse). Diapause blastocysts were recovered by flushing uteri 4 d after ovariectomy.

E6.5 postimplantation embryos were obtained via natural mating. The embryos were dissected from decidua in 10% FBS/ PBS(-). Reichert's membrane and the primitive endoderm were removed surgically using fine forceps. The ectoplacental cone (EPC) was cut off and embryos were separated into extraembryonic ectoderm (ExE) and epiblast (Epi).

The cells and tissues collected were stored at -80°C until use.

Cell culture. TS cell (established in our laboratory) and ES cell (MS12),[60] lines of C57BL/6 background were used in this study. Cells were maintained as described previously in reference 61 and 62.

Human samples. Human tissues were collected with permission from the Local Research Ethics Committees of the National Center for Child Health and Development. Written informed consent was obtained from all subjects. Chorionic villi were obtained after elective termination of normal pregnancies under 14 weeks of gestation. Placental tissues were obtained from normal-term pregnancies after delivery. Samples were snap-frozen for RNA and DNA isolation.

Genomic DNA samples of human ES cell lines (khES1, khES2 and khES3) were provided by Dr. Nakatsuji (Kyoto University).

Screening of TS-ES T-DMRs from the MSRE-qPCR data set. *NotI* sites to be analyzed by bisulfite sequencing in TS and ES cells were selected from the MSRE-qPCR data set (unpublished data and ref. 34). The detailed procedure used for MSRE-qPCR analysis was described previously in reference 34. Briefly, genomic DNA was incubated in the presence or absence of the methylation-sensitive restriction enzyme *NotI* prior to genomic qPCR flanking a *NotI* site of interest. The methylation level at each *NotI* site was estimated by the ratio of the amount of PCR product from *NotI*-treated DNA to that from the *NotI*-untreated DNA. In this study, potential TS-ES T-DMRs were selected using the following criteria: >35% methylation in undifferentiated/differentiated TS cells and ≤35% methylation in ES and EG cells, or vice versa. All resulting *NotI* sites appeared to be hypermethylated in TS cells. Among these *NotI* sites, we were able to design primer sets for bisulfite sequencing analysis for 14 loci.

Bisulfite sequencing analysis. With the exception of TS and ES cells, bisulfite treatment of genomic DNA was performed using the EZ DNA Methylation-Direct kit (Zymo Research, D5020). Genomic DNA from TS and ES cells was purified and then subjected to the bisulfite reaction using the kit. The procedures were performed according to the manufacturer's instructions, with a slight modification. Briefly, the last centrifugation step before elution was performed twice, to dry the column completely, and the elution solution was preheated to 50–60°C. PCR was performed using BIOTAQ HS DNA Polymerase (BIOLINE, BIO-21040) with the following parameters: 95°C for 10 min, 43 cycles of 95°C for 30 sec, 55°C (or 58°C) for 30 sec, and 72°C for 60 sec, followed by a step of 72°C for 2 min. The sequences of the PCR primers and annealing temperatures used are listed in **Table S5**. Bisulfite-treated DNA equivalent to approximately 100 TE or ICM cells, two blastocysts or 2.5–10 ng of genomic DNA was used as a template. For human samples, genomic DNA extracted from human ES cells and placenta was bisulfite treated using the EpiTect Bisulfite kit (QIAGEN, 59104), and an aliquot corresponding to 50 ng of untreated genomic DNA was used in one PCR.

The PCR products were purified, cloned into the pGEM-T Easy vector (Promega, A1360), and sequenced. Sequence analyses and statistical comparisons (nonparametric two-tailed Mann-Whitney test) were performed using the QUMA web service (quma.cdb.riken.jp).[63]

Disclosure of Potential Conflicts of Interest

No potential conflicts of interest were disclosed.

Acknowledgments

We thank Dr. Norio Nakatsuji for providing the genomic DNA of human ES cell lines. We also thank Dr. Shintaro Yagi for valuable discussions. This work was supported by a Grant-in-Aid for Scientific Research from the Ministry of Education, Culture, Sports, Science and Technology of Japan [20062003 (S.T.)].

Note

Supplemental materials can be found at:
www.landesbioscience.com/journals/epi/article/18962

References

1. Imamura T, Ohgane J, Ito S, Ogawa T, Hattori N, Tanaka S, et al. CpG island of rat sphingosine kinase-1 gene: tissue-dependent DNA methylation status and multiple alternative first exons. Genomics 2001; 76:117-25; PMID:11560121; http://dx.doi.org/10.1006/geno.2001.6607.
2. De Bustos C, Ramos E, Young JM, Tran RK, Menzel U, Langford CF, et al. Tissue-specific variation in DNA methylation levels along human chromosome 1. Epigenetics Chromatin 2009; 2:7; PMID:19505295; http://dx.doi.org/10.1186/1756-8935-2-7.
3. Shiota K, Kogo Y, Ohgane J, Imamura T, Urano A, Nishino K, et al. Epigenetic marks by DNA methylation specific to stem, germ and somatic cells in mice. Genes Cells 2002; 7:961-9; PMID:12296826; http://dx.doi.org/10.1046/j.1365-2443.2002.00574.x.
4. Cross JC, Werb Z, Fisher SJ. Implantation and the placenta: key pieces of the development puzzle. Science 1994; 266:1508-18; PMID:7985020; http://dx.doi.org/10.1126/science.7985020.
5. Manes C, Menzel P. Demethylation of CpG sites in DNA of early rabbit trophoblast. Nature 1981; 293:589-90; PMID:6270567; http://dx.doi.org/10.1038/293589a0.
6. Chapman V, Forrester L, Sanford J, Hastie N, Rossant J. Cell lineage-specific undermethylation of mouse repetitive DNA. Nature 1984; 307:284-6; PMID:6694730; http://dx.doi.org/10.1038/307284a0.
7. Razin A, Webb C, Szyf M, Yisraeli J, Rosenthal A, Naveh-Many T, et al. Variations in DNA methylation during mouse cell differentiation in vivo and in vitro. Proc Natl Acad Sci USA 1984; 81:2275-9; PMID:6585800; http://dx.doi.org/10.1073/pnas.81.8.2275.
8. Sanford JP, Clark HJ, Chapman VM, Rossant J. Differences in DNA methylation during oogenesis and spermatogenesis and their persistence during early embryogenesis in the mouse. Genes Dev 1987; 1:1039-46; PMID:3428592; http://dx.doi.org/10.1101/gad.1.10.1039.
9. Santos F, Hendrich B, Reik W, Dean W. Dynamic reprogramming of DNA methylation in the early mouse embryo. Dev Biol 2002; 241:172-82; PMID:11784103; http://dx.doi.org/10.1006/dbio.2001.0501.
10. Dean W, Santos F, Reik W. Epigenetic reprogramming in early mammalian development and following somatic nuclear transfer. Semin Cell Dev Biol 2003; 14:93-100; PMID:12524012; http://dx.doi.org/10.1016/S1084-9521(02)00141-6.
11. Santos F, Dean W. Epigenetic reprogramming during early development in mammals. Reproduction 2004; 127:643-51; PMID:15175501; http://dx.doi.org/10.1530/rep.1.00221.
12. Morgan HD, Santos F, Green K, Dean W, Reik W. Epigenetic reprogramming in mammals. Hum Mol Genet 2005; 14:47-58; PMID:15809273; http://dx.doi.org/10.1093/hmg/ddi114.
13. Howlett SK, Reik W. Methylation levels of maternal and paternal genomes during preimplantation development. Development 1991; 113:119-27; PMID:1764989.
14. Lane N, Dean W, Erhardt S, Hajkova P, Surani A, Walter J, et al. Resistance of IAPs to methylation reprogramming may provide a mechanism for epigenetic inheritance in the mouse. Genesis 2003; 35:88-93; PMID:12533790; http://dx.doi.org/10.1002/gene.10168.
15. Ko YG, Nishino K, Hattori N, Arai Y, Tanaka S, Shiota K. Stage-by-stage change in DNA methylation status of Dnmt1 locus during mouse early development. J Biol Chem 2005; 280:9627-34; PMID:15634679; http://dx.doi.org/10.1074/jbc.M413822200.
16. Yamagata K, Yamazaki T, Miki H, Ogonuki N, Inoue K, Ogura A, et al. Centromeric DNA hypomethylation as an epigenetic signature discriminates between germ and somatic cell lineages. Dev Biol 2007; 312:419-26; PMID:17964565; http://dx.doi.org/10.1016/j.ydbio.2007.09.041.
17. Iqbal K, Jin SG, Pfeifer GP, Szabó PE. Reprogramming of the paternal genome upon fertilization involves genome-wide oxidation of 5-methylcytosine. Proc Natl Acad Sci USA 2011; 108:3642-7; PMID:21321204; http://dx.doi.org/10.1073/pnas.1014033108.
18. Wossidlo M, Nakamura T, Lepikhov K, Marques CJ, Zakhartchenko V, Boiani M, et al. 5-Hydroxymethylcytosine in the mammalian zygote is linked with epigenetic reprogramming. Nat Commun 2011; 2:241; PMID:21407207; http://dx.doi.org/10.1038/ncomms1240.
19. Tanaka S, Kunath T, Hadjantonakis AK, Nagy A, Rossant J. Promotion of trophoblast stem cell proliferation by FGF4. Science 1998; 282:2072-5; PMID:9851926; http://dx.doi.org/10.1126/science.282.5396.2072.
20. Evans MJ, Kaufman MH. Establishment in culture of pluripotential cells from mouse embryos. Nature 1981; 292:154-6; PMID:7242681; http://dx.doi.org/10.1038/292154a0.
21. Martin GR. Isolation of a pluripotent cell line from early mouse embryos cultured in medium conditioned by teratocarcinoma stem cells. Proc Natl Acad Sci USA 1981; 78:7634-8; PMID:6950406; http://dx.doi.org/10.1073/pnas.78.12.7634.
22. Donnison M, Beaton A, Davey HW, Broadhurst R, L'Huillier P, Pfeffer PL. Loss of the extraembryonic ectoderm in Elf5 mutants leads to defects in embryonic patterning. Development 2005; 132:2299-308; PMID:15829518; http://dx.doi.org/10.1242/dev.01819.
23. Ng RK, Dean W, Dawson C, Lucifero D, Madeja Z, Reik W, et al. Epigenetic restriction of embryonic cell lineage fate by methylation of Elf5. Nat Cell Biol 2008; 10:1280-90; PMID:18836439; http://dx.doi.org/10.1038/ncb1786.
24. Nichols J, Zevnik B, Anastassiadis K, Niwa H, Klewe-Nebenius D, Chambers I, et al. Formation of pluripotent stem cells in the mammalian embryo depends on the POU transcription factor Oct4. Cell 1998; 95:379-91; PMID:9814708; http://dx.doi.org/10.1016/S0092-8674(00)81769-9.
25. Niwa H, Miyazaki J, Smith AG. Quantitative expression of Oct-3/4 defines differentiation, dedifferentiation or self-renewal of ES cells. Nat Genet 2000; 24:372-6; PMID:10742100; http://dx.doi.org/10.1038/74199.
26. Chambers I, Colby D, Robertson M, Nichols J, Lee S, Tweedie S, et al. Functional expression cloning of Nanog, a pluripotency sustaining factor in embryonic stem cells. Cell 2003; 113:643-55; PMID:12787505; http://dx.doi.org/10.1016/S0092-8674(03)00392-1.
27. Mitsui K, Tokuzawa Y, Itoh H, Segawa K, Murakami M, Takahashi K, et al. The homeoprotein Nanog is required for maintenance of pluripotency in mouse epiblast and ES cells. Cell 2003; 113:631-42; PMID:12787504; http://dx.doi.org/10.1016/S0092-8674(03)00393-3.
28. Hattori N, Nishino K, Ko YG, Hattori N, Ohgane J, Tanaka S, et al. Epigenetic control of mouse Oct-4 gene expression in embryonic stem cells and trophoblast stem cells. J Biol Chem 2004; 279:17063-9; PMID:14761969; http://dx.doi.org/10.1074/jbc.M309002200.
29. Hattori N, Imao Y, Nishino K, Hattori N, Ohgane J, Yagi S, et al. Epigenetic regulation of Nanog gene in embryonic stem and trophoblast stem cells. Genes Cells 2007; 12:387-96; PMID:17352742; http://dx.doi.org/10.1111/j.1365-2443.2007.01058.x.
30. Gidekel S, Bergman Y. A unique developmental pattern of Oct-3/4 DNA methylation is controlled by a cis-demodification element. J Biol Chem 2002; 277:34521-30; PMID:12110668; http://dx.doi.org/10.1074/jbc.M203338200.
31. Farthing CR, Ficz G, Ng RK, Chan CF, Andrews S, Dean W, et al. Global mapping of DNA methylation in mouse promoters reveals epigenetic reprogramming of pluripotency genes. PLoS Genet 2008; 4:1000116; PMID:18584034; http://dx.doi.org/10.1371/journal.pgen.1000116.
32. Yagi S, Hirabayashi K, Sato S, Li W, Takahashi Y, Hirakawa T, et al. DNA methylation profile of tissue-dependent and differentially methylated regions (T-DMRs) in mouse promoter regions demonstrating tissue-specific gene expression. Genome Res 2008; 18:1969-78; PMID:18971312; http://dx.doi.org/10.1101/gr.074070.107.
33. Takasugi M, Yagi S, Hirabayashi K, Shiota K. DNA methylation status of nuclear-encoded mitochondrial genes underlies the tissue-dependent mitochondrial functions. BMC Genomics 2010; 11:481; PMID:20723256; http://dx.doi.org/10.1186/1471-2164-11-481.
34. Sakamoto H, Suzuki M, Abe T, Hosoyama T, Himeno E, Tanaka S, et al. Cell type-specific methylation profiles occurring disproportionately in CpG-less regions that delineate developmental similarity. Genes Cells 2007; 12:1123-32; PMID:17903172; http://dx.doi.org/10.1111/j.1365-2443.2007.01120.x.
35. Wakayama S, Jakt ML, Suzuki M, Araki R, Hikichi T, Kishigami S, et al. Equivalency of nuclear transfer-derived embryonic stem cells to those derived from fertilized mouse blastocysts. Stem Cells 2006; 24:2023-33; PMID:16690779; http://dx.doi.org/10.1634/stemcells.2005-0537.
36. Oda M, Tanaka S, Yamazaki Y, Ohta H, Iwatani M, Suzuki M, et al. Establishment of trophoblast stem cell lines from somatic cell nuclear-transferred embryos. Proc Natl Acad Sci USA 2009; 106:16293-7; PMID:19706390; http://dx.doi.org/10.1073/pnas.0908009106.
37. Uy GD, Downs KM, Gardner RL. Inhibition of trophoblast stem cell potential in chorionic ectoderm coincides with occlusion of the ectoplacental cavity in the mouse. Development 2002; 129:3913-24; PMID:12135928.
38. Tomikawa J, Fukatsu K, Tanaka S, Shiota K. DNA methylation-dependent epigenetic regulation of dimethylarginine dimethylaminohydrolase 2 gene in trophoblast cell lineage. J Biol Chem 2006; 281:12163-9; PMID:16520373; http://dx.doi.org/10.1074/jbc.M513782200.
39. Hirasawa R, Chiba H, Kaneda M, Tajima S, Li E, Jaenisch R, et al. Maternal and zygotic Dnmt1 are necessary and sufficient for the maintenance of DNA methylation imprints during preimplantation development. Genes Dev 2008; 22:1607-16; PMID:18559477; http://dx.doi.org/10.1101/gad.1667008.
40. Borgel J, Guibert S, Li Y, Chiba H, Schübeler D, Sasaki H, et al. Targets and dynamics of promoter DNA methylation during early mouse development. Nat Genet 2010; 42:1093-100; PMID:21057502; http://dx.doi.org/10.1038/ng.708.
41. Dietrich JE, Hiiragi T. Stochastic patterning in the mouse pre-implantation embryo. Development 2007; 134:4219-31; PMID:17978007; http://dx.doi.org/10.1242/dev.003798.
42. Pearton DJ, Broadhurst R, Donnison M, Pfeffer PL. Elf5 regulation in the trophectoderm. Dev Biol 2011; 360:343-50; PMID:22020251; http://dx.doi.org/10.1016/j.ydbio.2011.10.007.
43. Sakaue M, Ohta H, Kumaki Y, Oda M, Sakaide Y, Matsuoka C, et al. DNA methylation is dispensable for the growth and survival of the extraembryonic lineages. Curr Biol 2010; 20:1452-7; PMID:20637626; http://dx.doi.org/10.1016/j.cub.2010.06.050.

44. O'Neill LP, VerMilyea MD, Turner BM. Epigenetic characterization of the early embryo with a chromatin immunoprecipitation protocol applicable to small cell populations. Nat Genet 2006; 38:835-41; PMID:16767102; http://dx.doi.org/10.1038/ng1820.
45. Torres-Padilla ME, Parfitt DE, Kouzarides T, Zernicka-Goetz M. Histone arginine methylation regulates pluripotency in the early mouse embryo. Nature 2007; 445:214-8; PMID:17215844; http://dx.doi.org/10.1038/nature05458.
46. Ikegami K, Ohgane J, Tanaka S, Yagi S, Shiota K. Interplay between DNA methylation, histone modification and chromatin remodeling in stem cells and during development. Int J Dev Biol 2009; 53:203-14; PMID:19412882; http://dx.doi.org/10.1387/ijdb.082741ki.
47. Murr R. Interplay between different epigenetic modifications and mechanisms. Adv Genet 2010; 70:101-41; PMID:20920747; http://dx.doi.org/10.1016/B978-0-12-380866-0.60005-8.
48. Reijo Pera RA, DeJonge C, Bossert N, Yao M, Hwa Yang JY, Asadi NB, et al. Gene expression profiles of human inner cell mass cells and embryonic stem cells. Differentiation 2009; 78:18-23; PMID:19398262; http://dx.doi.org/10.1016/j.diff.2009.03.004.
49. Tang F, Barbacioru C, Bao S, Lee C, Nordman E, Wang X, et al. Tracing the derivation of embryonic stem cells from the inner cell mass by single-cell RNA-Seq analysis. Cell Stem Cell 2010; 6:468-78; PMID:20452321; http://dx.doi.org/10.1016/j.stem.2010.03.015.
50. Wongtawan T, Taylor JE, Lawson KA, Wilmut I, Pennings S. Histone H4K20me3 and HP1α are late heterochromatin markers in development, but present in undifferentiated embryonic stem cells. J Cell Sci 2011; 124:1878-90; PMID:21576353; http://dx.doi.org/10.1242/jcs.080721.
51. Dean W, Santos F, Stojkovic M, Zakhartchenko V, Walter J, Wolf E, et al. Conservation of methylation reprogramming in mammalian development: aberrant reprogramming in cloned embryos. Proc Natl Acad Sci USA 2001; 98:13734-8; PMID:11717434; http://dx.doi.org/10.1073/pnas.241522698.
52. Bonk AJ, Li R, Lai L, Hao Y, Liu Z, Samuel M, et al. Aberrant DNA methylation in porcine in vitro-, parthenogenetic- and somatic cell nuclear transfer-produced blastocysts. Mol Reprod Dev 2008; 75:250-64; PMID:17595009; http://dx.doi.org/10.1002/mrd.20786.
53. Abell AN, Granger DA, Johnson NL, Vincent-Jordan N, Dibble CF, Johnson GL. Trophoblast stem cell maintenance by fibroblast growth factor 4 requires MEKK4 activation of Jun N-terminal kinase. Mol Cell Biol 2009; 29:2748-61; PMID:19289495; http://dx.doi.org/10.1128/MCB.01391-08.
54. Fazzari MJ, Greally JM. Epigenomics: beyond CpG islands. Nat Rev Genet 2004; 5:446-55; PMID:15153997; http://dx.doi.org/10.1038/nrg1349.
55. Coulondre C, Miller JH, Farabaugh PJ, Gilbert W. Molecular basis of base substitution hotspots in *Escherichia coli*. Nature 1978; 274:775-80; PMID:355893; http://dx.doi.org/10.1038/274775a0.
56. Rossant J, Sanford JP, Chapman VM, Andrews GK. Undermethylation of structural gene sequences in extraembryonic lineages of the mouse. Dev Biol 1986; 117:567-73; PMID:2428685; http://dx.doi.org/10.1016/0012-1606(86)90325-8.
57. Ohgane J, Hattori N, Oda M, Tanaka S, Shiota K. Differentiation of trophoblast lineage is associated with DNA methylation and demethylation. Biochem Biophys Res Commun 2002; 290:701-6; PMID:11785956; http://dx.doi.org/10.1006/bbrc.2001.6258.
58. Fulka H, Mrazek M, Tepla O, Fulka J Jr. DNA methylation pattern in human zygotes and developing embryos. Reproduction 2004; 128:703-8; PMID:15579587; http://dx.doi.org/10.1530/rep.1.00217.
59. Nagy A, Gertstensen M, Vintersten K, Behringer R. Manipulating the Mouse Embryo. New York: Cold Spring Harbor Laboratory Press 2003.
60. Kawase E, Suemori H, Takahashi N, Okazaki K, Hashimoto K, Nakatsuji N. Strain difference in establishment of mouse embryonic stem (ES) cell lines. Int J Dev Biol 1994; 38:385-90; PMID:7981049.
61. Oda M, Shiota K, Tanaka S. Trophoblast stem cells. Methods Enzymol 2006; 419:387-400; PMID:17141063; http://dx.doi.org/10.1016/S0076-6879(06)19015-1.
62. Matise MP, Auerbach W, Joyner AL. Gene targeting: A Practical Approach Second Edition. New York: Oxford University Press 2000.
63. Kumaki Y, Oda M, Okano M. QUMA: quantification tool for methylation analysis. Nucleic Acids Res 2008; 36:170-5; PMID:18487274; http://dx.doi.org/10.1093/nar/gkn294.

Contribution of Intragenic DNA Methylation in Mouse Gametic DNA Methylomes to Establish Oocyte-Specific Heritable Marks

Hisato Kobayashi[1], Takayuki Sakurai[1], Misaki Imai[2], Nozomi Takahashi[1], Atsushi Fukuda[1], Obata Yayoi[1], Shun Sato[3], Kazuhiko Nakabayashi[3], Kenichiro Hata[3], Yusuke Sotomaru[4], Yutaka Suzuki[5], Tomohiro Kono[1,2]*

1 Department of BioScience, Tokyo University of Agriculture, Tokyo, Japan, **2** Genome Research Center, NODAI Research Institute, Tokyo University of Agriculture, Tokyo, Japan, **3** Department of Maternal-Fetal Biology, National Research Institute for Child Health and Development, Tokyo, Japan, **4** Natural Science Center for Basic Research and Development, Hiroshima University, Hiroshima, Japan, **5** Department of Medical Genome Sciences, Graduate School of Frontier, The University of Tokyo, Kashiwa, Japan

Abstract

Genome-wide dynamic changes in DNA methylation are indispensable for germline development and genomic imprinting in mammals. Here, we report single-base resolution DNA methylome and transcriptome maps of mouse germ cells, generated using whole-genome shotgun bisulfite sequencing and cDNA sequencing (mRNA-seq). Oocyte genomes showed a significant positive correlation between mRNA transcript levels and methylation of the transcribed region. Sperm genomes had nearly complete coverage of methylation, except in the CpG-rich regions, and showed a significant negative correlation between gene expression and promoter methylation. Thus, these methylome maps revealed that oocytes and sperms are widely different in the extent and distribution of DNA methylation. Furthermore, a comparison of oocyte and sperm methylomes identified more than 1,600 CpG islands differentially methylated in oocytes and sperm (germline differentially methylated regions, gDMRs), in addition to the known imprinting control regions (ICRs). About half of these differentially methylated DNA sequences appear to be at least partially resistant to the global DNA demethylation that occurs during preimplantation development. In the absence of *Dnmt3L*, neither methylation of most oocyte-methylated gDMRs nor intragenic methylation was observed. There was also genome-wide hypomethylation, and partial methylation at particular retrotransposons, while maintaining global gene expression, in oocytes. Along with the identification of the many *Dnmt3L*-dependent gDMRs at intragenic regions, the present results suggest that oocyte methylation can be divided into 2 types: *Dnmt3L*-dependent methylation, which is required for maternal methylation imprinting, and *Dnmt3L*-independent methylation, which might be essential for endogenous retroviral DNA silencing. The present data provide entirely new perspectives on the evaluation of epigenetic markers in germline cells.

Citation: Kobayashi H, Sakurai T, Imai M, Takahashi N, Fukuda A, et al. (2012) Contribution of Intragenic DNA Methylation in Mouse Gametic DNA Methylomes to Establish Oocyte-Specific Heritable Marks. PLoS Genet 8(1): e1002440. doi:10.1371/journal.pgen.1002440

Editor: Wolf Reik, The Babraham Institute, United Kingdom

Received July 28, 2011; **Accepted** November 14, 2011; **Published** January 5, 2012

Funding: This work was supported by Grants-in-Aid for Scientific Research from the Ministry of Education, Science, Sports, and Culture of Japan (Grant Nos. 222228004, 20062009, 221S0002, S0801025). The funders had no role in study design, data collection and analysis, decision to publish, or preparation of the manuscript.

Competing Interests: The authors have declared that no competing interests exist.

* E-mail: tomohiro@nodai.ac.jp

Introduction

Throughout mammalian gametogenesis, dynamic DNA methylation changes occur in a sex- and sequence-specific manner. These changes result in the establishment of oocyte- and sperm-specific genomic imprints and unique methylation patterns of repetitive elements via DNA methyltransferase activity [1–4]. This process is indispensable for functional gamete and embryo development. For example, sex-specific methylation imprints are maintained throughout cell division after fertilization, despite genome-wide demethylation and *de novo* methylation during embryogenesis. These imprints control parent-of-origin specific monoallelic expression of a subset of genes, which are known as imprinted genes [5–9]. In addition, DNA methylation during spermatogenesis plays a crucial role in meiotic progression and retrotransposon silencing [10–14]. However, little is known about the profile and functional role of DNA methylation during oogenesis, except for the establishment of genomic imprints.

Recently, the epigenetic modifications which are responsible for regulating cell differentiation and embryo development have been studied in detail by using high-throughput sequencing: bisulfite sequencing ("BS-seq"); "Methyl-seq" with a methyl-sensitive restriction enzyme; "MeDIP-seq" with methylated DNA immunoprecipitation; and "MBD-seq" with a methyl-DNA binding domain protein antibody [15–26]. However, a major limitation of epigenomic studies is the lack of a standard methodology for DNA methylome analysis. Ideally, the gold standard is high resolution and genome-wide methylome analysis of germ cells. However, genome-wide methylome analysis of female germ cells has almost never been performed due to the limited availability of samples.

Author Summary

In mammals, germ-cell–specific methylation patterns and genomic imprints are established throughout large-scale de novo DNA methylation in oogenesis and spermatogenesis. These steps are required for normal germline differentiation and embryonic development; however, current DNA methylation analyses only provide us a partial picture of germ cell methylome. To the best of our knowledge, this is the first study to generate comprehensive maps of DNA methylomes and transcriptomes at single base resolution for mouse germ cells. These methylome maps revealed genome-wide opposing DNA methylation patterns and differential correlation between methylation and gene expression levels in oocyte and sperm genomes. In addition, our results indicate the presence of 2 types of methylation patterns in the oocytes: (i) methylation across the transcribed regions, which might be required for the establishment of maternal methylation imprints and normal embryogenesis, and (ii) retroviral methylation, which might be essential for silencing of retrotransposons and normal oogenesis. We believe that an extension of this work would lead to a better understanding of the epigenetic reprogramming in germline cells and of the role for gene regulations.

Shotgun bisulfite sequencing (SBS) may be able to overcome this limitation and enable the determination of the cytosine methylation status of individual CpG sites at a whole-genome level without a bias toward CpG-rich regions [22,23,26] and with only relatively small-scale DNA samples [24,27]. As a result, in this study, an improved SBS method for small-scale DNA samples was used to analyze the DNA methylome of mouse germ cells. In addition, the mouse germ cell transcriptome was investigated using high-throughput cDNA sequencing (mRNA-seq) to reveal relationships between DNA methylation and gene transcription in both male and female germ cells.

Results

Genome sequencing

We performed SBS analysis by using MethylC-seq [22] and a new SBS method called "whole bisulfitome-amplified DNA sequencing" (WBA-seq). The MethylC-seq and WBA-seq libraries were generated as shown in Figure S1. The MethylC-seq method generated 1010 and 1085 million tags (reads) from germinal vesicle (GV) stage oocytes and epididymal sperm, respectively. Oocyte DNA libraries generated by MethylC-seq showed higher redundancies than sperm DNA libraries. For example, 33.0% and 81.7% of the 21 million cytosines of CpGs in the mouse genome were covered by at least 1 sequence read from GV oocytes and sperm, respectively; whereas the average read depth (*i.e.*, the number of hits of reads that were mapped to a given position) was over 10× for both germ cells (Figure S2). The WBA-seq method generated 307 and 397 million tags from GV oocytes obtained from wild-type and *Dnmt3L*-deficient (*Dnmt3L*$^{-/-}$) mice, respectively. WBA-seq libraries for GV oocytes showed higher genome coverage (60% of genomic CpGs were covered by at least 1 read) but with smaller average read depth (7.4×) than MethylC-seq library. Some reads from the oocyte libraries strongly matched mitochondrial DNA (mtDNA), satellite, low complexity, or simple repeat sequences (Figure S3), which might have been due to a distinct genomic copy number bias in the mitochondria of germ cells or an over-amplification bias. Thus, SBS results were simplified by removing the redundancy information (only mtDNA was separately examined for DNA methylation) and combining MethylC-seq and WBA-seq results for wild-type oocytes. Consequently, the average read depth was 18.8×, 4.4×, and 12.5× for wild-type and *Dnmt3L*$^{-/-}$ oocytes, and sperm, respectively, and 70.8%, 45.6%, and 79.9% of genomic CpGs were covered by at least 1 sequence read from each cell type (Table 1 and Figure S3). Furthermore, the average read depths of MethylC-seq of mouse blastocysts and embryonic stem cells (ESCs), which served as zygote and stem cell controls, were 12.8× and 6.1×, respectively (Table 1).

Methylome of mouse germ cells

The average methylation level of wild-type oocytes (40.0%) was less than half that of sperm (89.4%) (Figure S4). This difference in global DNA methylation between male and female germ cells was consistent with results from the previous studies [28,29]. The *Dnmt3L*$^{-/-}$ oocyte genome was observed to be hypomethylated, exhibiting a methylation level of only 5.5%. Furthermore, blastocysts showed a lesser extent of methylation (21.3%) than did wild-type oocytes; ESCs, on the other hand, showed relatively high levels of methylation (70.6%). To elucidate the distribution of methylation levels on CpG sites, on regional and genome-wide scales, we created dot plots of CpG methylation for individual chromosomes and histograms of the methylation levels for all CpGs. These graphs revealed that hypermethylated CpGs in oocytes tended to cluster in transcribed regions of particular genes (*e.g.*, *Kcnq1* or *Rlim* genes, known to be expressed in oocytes [30,31]); the sperm genome was almost entirely hypermethylated, except at most CpG-rich regions (Figure 1 and Figure S5). Specifically, 55.7% of the CpGs in the oocyte genome exhibited <10% methylation, whereas another 32.0% of CpGs exhibited ≥90% methylation (Figure 2A). The *Dnmt3L*$^{-/-}$ oocyte genome was also hypomethylated in almost all chromosomal regions (Figure S6). The methylation level of the mtDNA genome in

Table 1. Summary of shotgun bisulfite sequencing data.

Sample	Method	Aligned tags (base)	Genome covarage		Read depth
			(>x1)	(>x5)	
Wild-type oocyte	MethylC-seq & WBA-seq	51,166,451,066	70.8%	39.4%	18.8
Dnmt3L$^{-/-}$ oocyte	WBA-seq	11,872,662,647	45.6%	19.6%	4.4
Sperm	MethylC-seq	34,153,237,944	79.9%	63.4%	12.5
Blastocyst	MethylC-seq	34,857,014,339	86.2%	79.4%	12.8
ESC	MethylC-seq	16,691,289,063	73.0%	38.9%	6.1

doi:10.1371/journal.pgen.1002440.t001

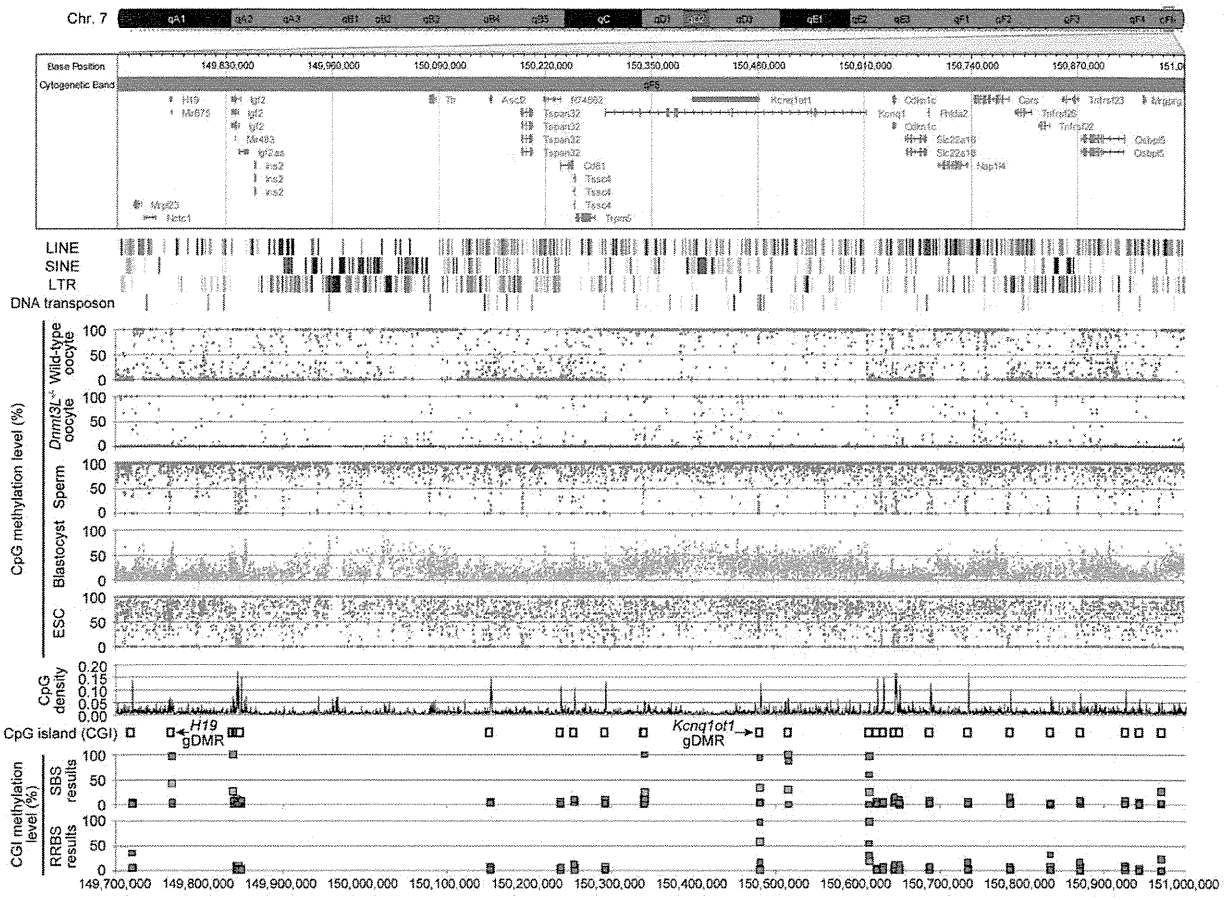

Figure 1. High-resolution DNA methylome map of mouse distal chromosome 7 imprinting cluster. Illumina GenomeStudio viewer displays the locations of genes in distal chromosome 7 (149,700,000–151,000,000). Black vertical bars represent the location of 4 repetitive elements: LINE, SINE, LTR, and DNA transposons. Red, purple, blue, green, and khaki dots represent the methylation levels at individual CpGs in wild-type oocyte, *Dnmt3L*$^{-/-}$ oocyte, sperm, blastocyst, and ESC genomes, respectively. Black line plots depict the distribution of CpG densities (number of CpG per 200 nt) of individual CpGs. Open boxes represent the location of CpG islands (CGIs). Red, purple, blue, and green boxes represent the methylation levels at individual CGIs in wild-type oocyte, *Dnmt3L*$^{-/-}$ oocyte, sperm, and blastocyst genomes, respectively, determined by our results from shotgun bisulfite sequencing (SBS) method and Smallwood's results from reduced representation bisulfite sequencing (RRBS) method [38].
doi:10.1371/journal.pgen.1002440.g001

Dnmt3L$^{-/-}$ oocytes (4.4%) was lower than that observed in wild-type oocytes (6.6%). Sperm methylation levels, by comparison, were relatively high (14.7%), whereas those of the blastocysts and ESCs were quite low (1.3% and 2.1%, respectively) (Figure S4).

Since previous studies revealed a significant correlation between CpG frequency and methylation within intra- and intergenic regions in somatic cells [32,33], the CpG density and methylation levels were compared to identify genome-wide differential methylation patterns in germ cells. CpG density was defined as the number of CpG dinucleotides in 200 nucleotide (nt) windows (*e.g.*, 1 CpG dinucleotide per 200 nt corresponds to a density of 0.005). At low CpG densities (range, 0.005–0.05), the oocyte genome was about 50% methylated, whereas the sperm genome was 80–90% methylated. At moderate to high CpG densities (range, 0.05–0.2), both male and female germ cells were hypomethylated (Figure 2B). Furthermore, 4 families of transposable elements (long interspersed nuclear elements (LINEs), short interspersed nuclear elements (SINEs), long terminal repeats (LTRs), and DNA transposons) were moderately methylated in oocyte genomes but were hypermethylated in sperm. In addition, a general trend towards higher methylation levels at higher CpG densities in the oocyte genome occurred in LTRs. Conversely, a trend toward lower CpG methylation levels at higher CpG densities in the wild-type oocyte and sperm genomes was observed in SINEs and DNA transposons. In contrast, all of these transposable elements were hypomethylated in *Dnmt3L*$^{-/-}$ oocytes. Interestingly, however, there was partial CpG methylation in LINEs and LTRs at relatively high CpG densities (range, 0.03–0.1). These complete or partial under-methylations were confirmed by bisulfite sequencing in L1 LINEs, B1/Alu SINEs, and intracisternal A particle (IAP) LTRs (Figure S7). These results suggested that each germ cell has a unique sequence- and CpG-density-dependent methylation pattern. In addition, oocyte CpG methylation, except in a subset of retrotransposons, appears to be *Dnmt3L* dependent.

We also characterized the methylation patterns of 15 germline-differentially methylated regions (gDMRs). The differential (between oocyte and sperm) methylation occurs at imprinted gene loci (also called imprinting control regions (ICRs)). The ICRs of maternally methylated imprinted genes (*e.g.*, *Nespas-Gnas*) were shown to be hypermethylated in oocytes but hypomethylated in sperm, while the converse was true in ICRs of paternally-methylated imprinted genes (*e.g.*, *H19*) (Figure 3 and Figure S8). Interestingly, only the *Snrpn*

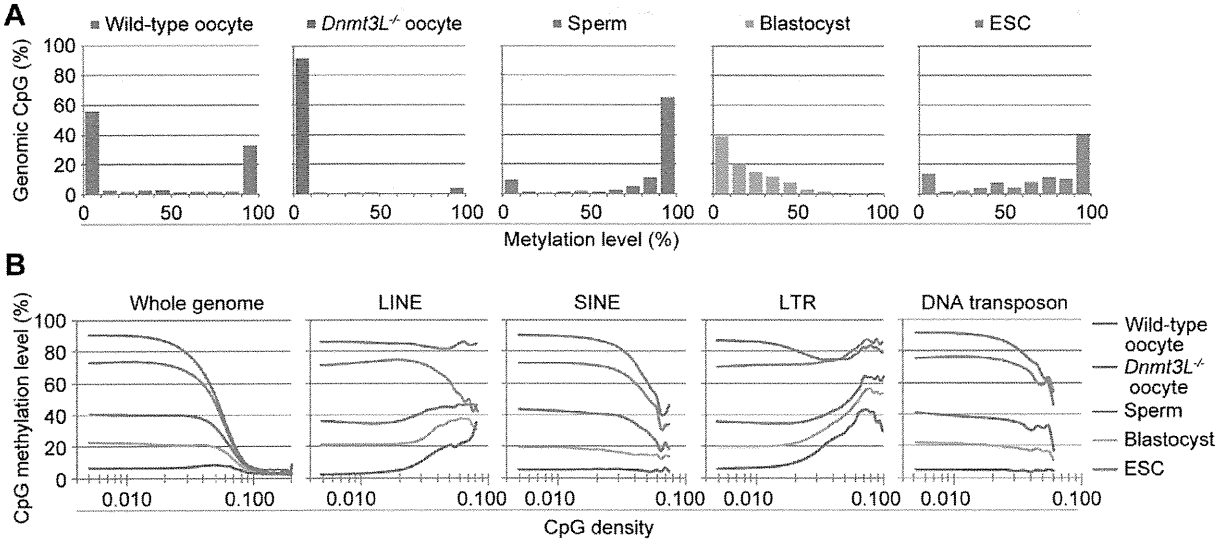

Figure 2. Genome-wide methylation profiling of mouse germ cells. (A) Histograms of methylation levels of genomic CpGs in wild-type oocyte, *Dnmt3L*$^{-/-}$ oocyte, sperm, blastocyst, and embryonic stem cell (ESC) genomes. (B) CpG methylation levels are plotted as a function of CpG density for the whole genome and 4 families of transposable elements (long interspersed nuclear element (LINE), short interspersed nuclear element (SINE), long terminal repeat (LTR), and DNA transposon).
doi:10.1371/journal.pgen.1002440.g002

gDMR was partially methylated (35.7%), whereas all other maternal ICRs were hypomethylated in *Dnmt3L*$^{-/-}$ oocytes (Table 2). This residual methylation might result in the stochastic acquisition of the maternal imprint in the progeny of *Dnmt3L*$^{-/-}$ females [34]. These results strongly suggested that the methylation level of individual CpGs can be determined from DNA methylome maps with a high degree of accuracy.

The study of mammalian DNA methylation patterns has previously suggested that methylation predominantly occurs at CpG sites; however, more recent studies, based on SBS methods, have indicated that methylation at non-CpG sites also occurs in human ESCs [22,23]. Detection of non-CpG methylation is one of the applications of the bisulfite-based methylation analysis but is problematic due to the incomplete conversion of cytosine, and overestimates of such cytosine by PCR amplification, which cannot be discriminated from true methylation. In order to evaluate the methylation status of non-CpG sites and avoid these problems, additional SBS analysis of mouse GV oocytes, sperm, blastocysts, and ESCs was performed by a non-amplification technique, termed Post-Bisulfite Adapter Tagging (PBAT) [Miura F. & Ito T, personal communication]. All C (originally methylated cytosine) and T (originally unmethylated cytosine) that mapped to genomic CpG and CpH sites (H = A, T, or C) were counted. The PBAT results showed CpG methylation ratios (C ratios = 0.395, 0.748, 0.137, 0.615 in oocytes, sperm. blastocysts, and ESCs) which are similar to the average methylation levels of individual DNA methylome maps obtained by MethylC-seq and WBA-seq among all examined cells. Interestingly, a relatively high fold enrichment of non-CpG methylation was observed in GV oocytes (C ratio = 0.034–0.038), but not in the other cell types, including mouse ESCs (C ratio <0.01) (Figure S11).

Relationship between the DNA methylome and transcriptome of mouse germ cells

To elucidate the interaction between intragenic DNA methylation and gene transcription, the correlation between promoter and gene-body methylation and expression levels for 20,854 different genes was examined. The mRNA-seq profiles for germ cells and ESCs are shown in Table S1. The results showed that mRNA transcript levels in oocytes were strongly correlated to gene-body methylation levels (Spearman's $\rho > 0.5$, $p < 1 \times 10^{-9}$) but were not significantly correlated to promoter methylation levels ($|\rho| < 0.1$) (Figure 4A). For example, the regions +2 to +5 kb from the transcription start site (TSS) and 0 to −5 kb from the transcription termination site (TTS) were hypermethylated (60–90% methylation) for the top 20% of expressed genes but were hypomethylated (10–30% methylation) for the bottom 20% of expressed genes. However, areas near the TSS (±500 base pairs (bp)) were hypomethylated (10–20% methylation) in all genes, regardless of their expression level. In contrast, in the *Dnmt3L*$^{-/-}$ oocyte genome, the correlation between gene expression and gene-body methylation was very weak ($|\rho| < 0.1$) (Figure 4B). In the sperm genome, promoter methylation was negatively correlated (Spearman's $\rho = -0.36$, $p < 1 \times 10^{-9}$) with gene expression, whereas gene-body methylation was positively correlated (Spearman's $\rho = 0.14$–0.16, $p < 1 \times 10^{-9}$) to gene expression; the latter correlation was weaker than that observed in the oocyte genome (Figure 4C).

Role of *Dnmt3L* in the DNA methylome/transcriptome relationship

Further investigation of gene expression patterns in oocyte genomes revealed that the mRNA transcript levels between wild-type and *Dnmt3L*$^{-/-}$ oocytes were very highly correlated ($R^2 = 0.9611$) (Figure 5A). In fact, there were no significant differences in the expression levels of representative oocyte-specific genes (*e.g.*, *Gdf9*, *Bmp15*, *Bcl2l10*, *Zp1*, *Zp2*, *Zp3*, *Zar1*, *Npm2*, *Nlrp5*, and *Dppa3*, which are responsible for ovarian follicle formation, reproduction, and early development [35]) and DNA methyltransferase genes (*e.g.*, *Dnmt1*, a maintenance methyltransferase, and *Dnmt3a* and *Dnmt3b de novo* methyltransferases); the expected difference in the expression level of *Dnmt3L* between wild-type and

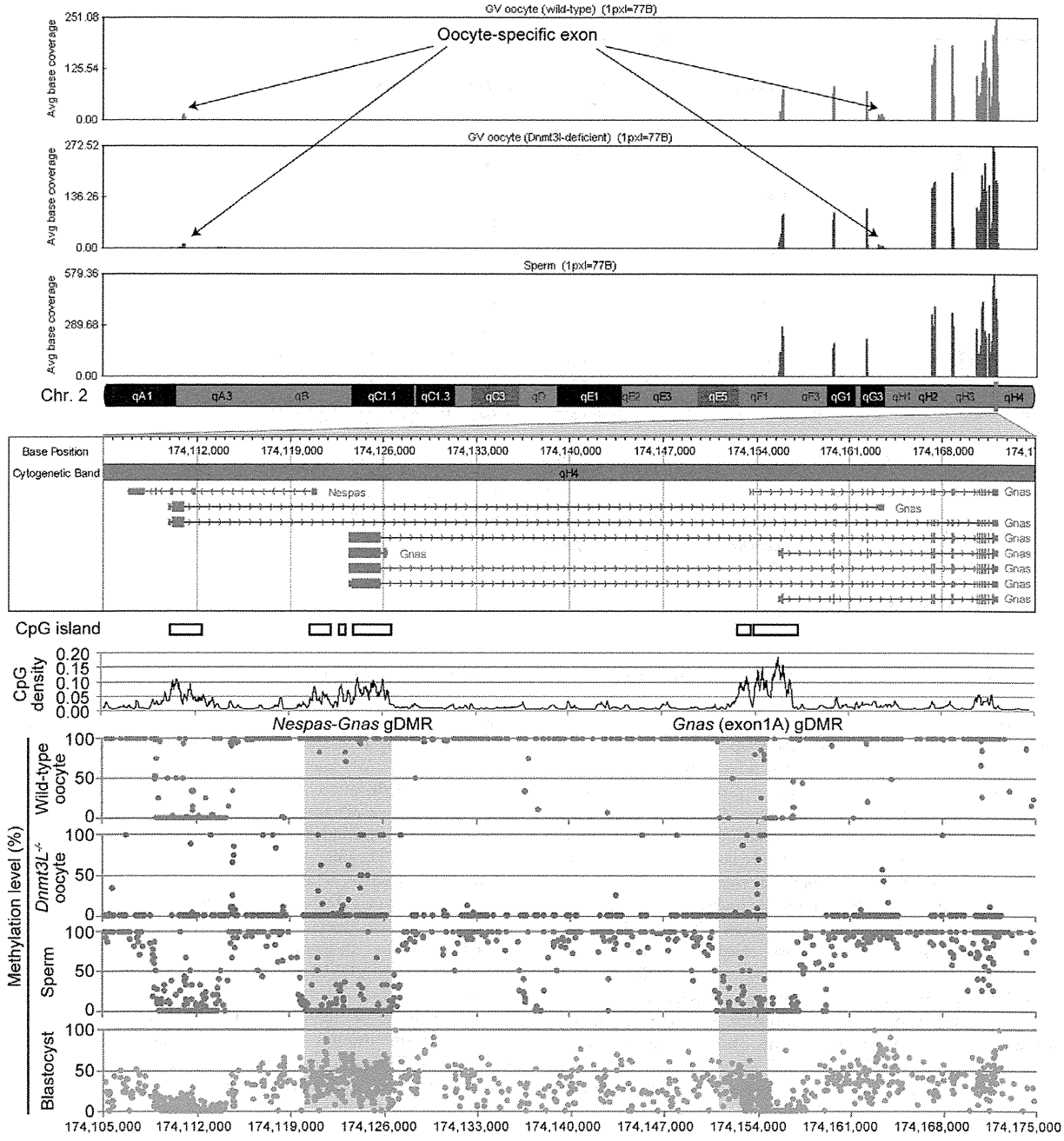

Figure 3. High-resolution genome-wide mRNA expression and CpG methylation profiling. GenomeStudio view of mRNA-seq data and CpG methylation map of the genomic region spanning the *Nespas-Gnas* maternally imprinted locus. (*Top*) Genomic stacked alignment plots of wild-type oocytes, *Dnmt3L*$^{-/-}$ oocytes, and sperm. (*Middle*) Open boxes and black line plots represent the location of CGIs and the distribution of CpG densities of individual CpGs, respectively. (*Bottom*) Red, purple, blue, and green dots represent the methylation levels at individual CpGs in wild-type oocyte, *Dnmt3L*$^{-/-}$ oocyte, sperm, and blastocyst genomes, respectively. The red shaded areas show the extent of two maternal imprinting control regions (ICRs).
doi:10.1371/journal.pgen.1002440.g003

Dnmt3L$^{-/-}$ oocytes was observed (Figure 5B, 5C). These results suggested that changes in gene expression did not occur during oogenesis, despite global intragenic hypomethylation in *Dnmt3L*$^{-/-}$ oocytes. Furthermore, the expression levels and exon patterns of maternally-methylated imprinted genes across each ICR were not altered in *Dnmt3L*$^{-/-}$ oocytes (Figure 3 and Figure 5D). This result suggested that the disruption of maternal methylation imprints in the *Dnmt3L*$^{-/-}$ oocyte genome was not due to the lack of their transcription [36]. On the other hand, maternal methylation imprints at ICRs (and many other hypermethyla-

Table 2. CpG methylation profiling of 12 maternal and 3 paternal imprinting control regions.

	Gene locus	Chr.	Extents of the ICRs†		Average methylation levels				
			Start	End	Wild-type oocyte	*DnmtLl*$^{-/-}$ oocyte	Sperm	Blastocyst	ESC
Maternally methylate imprinted genes	*Nespas-Gnas*	2	174,119,863	174,126,564	99.3%	5.6%	3.9%	38.2%	55.9%
	Gnas (exon1A)	2	174,150,877	174,154,638	95.2%	3.5%	4.1%	20.4%	7.8%
	Peg10	6	4,696,743	4,699,483	95.9%	6.7%	5.5%	31.8%	57.1%
	Mest	6	30,684,932	30,689,966	96.5%	2.3%	4.2%	30.7%	52.6%
	Peg3	7	6,679,787	6,684,257	98.1%	3.0%	2.5%	32.1%	42.8%
	Snrpn	7	67,147,381	67,151,583	94.1%	35.7%	4.6%	34.3%	64.9%
	Kcnq1ot1	7	150,480,736	150,482,810	97.9%	2.2%	4.3%	34.1%	52.0%
	Plagl1	10	12,809,697	12,812,131	99.9%	1.3%	7.4%	35.4%	53.0%
	Grb10	11	11,925,127	11,927,100	98.0%	1.2%	5.3%	38.5%	78.7%
	Zrsr1	11	22,871,610	22,874,212	94.1%	5.2%	6.8%	34.8%	47.0%
	Igf2r	17	12,934,169	12,935,816	99.1%	0.9%	3.8%	44.2%	53.2%
	Impact	18	13,130,435	13,133,510	97.2%	2.4%	6.6%	43.1%	38.6%
Paternally methylated imprinted genes	*H19*	7	149,764,673	149,771,930	13.5%	0.6%	96.5%	40.8%	65.5%
	Rasgrf1	9	89,767,090	89,775,128	7.4%	0.7%	92.0%	25.2%	59.4%
	Dlk1-Meg3	12	110,762,703	110,773,093	18.9%	0.9%	96.8%	32.4%	83.1%

†: The extents of each region in germ cells were determined by bisulfite sequencing study [39].

doi:10.1371/journal.pgen.1002440.t002

tions at transcribed regions) in wild-type oocyte genomes might be the result of gene transcription via *Dnmt3L*-mediated intragenic methylation.

Surprisingly, gene expression in ESC genomes was negatively correlated with promoter methylation and was not positively correlated with gene-body methylation (Figure S12). Meanwhile, these ESCs showed the apparent expression of all DNA methyltransferase gene families including *Dnmt3L* (Figure S13). Previous studies indicated that the zygotic and somatic functioning of *Dnmt3L* is not essential for global methylation in ESCs in mice [6]. Thus, unlike oocytes, the functional role of *Dnmt3L* in gene-body methylation after fertilization is unclear. However, the expression of pluripotency-associated genes, *Pou5f1*, *Klf4*, *Sox2*, *Myc*, *Nanog*, and *Lin28a*, was clearly observed in ESCs. The expression of *Pou5f1*, *Lin28a*, and *Glis1*, recently identified as maternal reprogramming factors, were also observed in oocytes (Figure S14). While differential expression of the pluripotency genes among germ and stem cells was observed, the promoter regions of these genes demonstrated low-level methylation in almost all of the examined cells. In sperm cells, only the *Nanog* promoter was hypermethylated (this result was similar to a previous study [29]).

Identification and characterization of germline differentially methylated regions

To identify gDMRs, the average CpG methylation levels of individual CpG islands (CGIs), which are CpG-rich genomic regions often lacking DNA methylation, were calculated. Recently, Illingworth et al. determined the number of CGIs by deep sequencing of isolated, unmethylated DNA clusters [37]. Among the 23,021 mouse CGIs (22,974 CGIs were informative in both oocytes and sperm), 2014 were highly methylated (≥80% methylation) in oocytes, 818 were highly methylated in sperm, and 377 were highly methylated in both germ cells (Figure 6A). Furthermore, we also identified 1678 gDMRs (≥80% methylation in 1 gamete and ≤20% in the other), 1329 of which were oocyte-specific methylated CGIs, while the remaining 349 were sperm-specific methylated CGIs (Figure 6A, Figure S6, and Table S2). Among these gDMRs, 646 gDMRs were confirmed to show a differential methylation status between GV oocytes and sperm (by similar criteria: ≥75% methylation in 1 gamete and ≤25% in the other); the methylation status was previously examined by performing large-scale bisulfite sequencing of CpG-rich regions of the genome (reduced representation bisulfite sequencing: RRBS) (Table S3) [38]. Additionally, almost all known ICRs except *Zdbf2* DMRs (which do not have any CGIs) were re-identified from our gDMR list (Table S2).

A total of 78% oocyte-methylated gDMRs (n = 1045) were located within the intragenic regions. Approximately 25% of the oocyte-methylated gDMRs (n = 322) overlap with either the first exon or the proximal promoter regions of the genes, as has been observed with most of the described maternal ICRs [39]; only 5% of the sperm-methylated gDMR (n = 18) showed such overlap. Alternatively, 34% of sperm-methylated gDMRs (n = 120) overlap with intergenic regions, as in all known paternal ICRs (Figure 6B). Interestingly, oocyte-methylated gDMRs in transcribed regions tended to be more abundant within highly expressed genes, but such a trend was not observed in the sperm genome (Figure 6C). Oocyte-methylated gDMRs were also identified in non-imprinted genes, such as the DNA methyltransferase genes (*e.g.*, *Dnmt1* and *Dnmt3b*) and some male germline-specific genes (*e.g.*, *Piwil1*, *Spag1*, *Ggnbp2*, *Tbpl1*, *Spata16*, *Ggn*, *Acrbp*, and *Cd46*). The oocyte-methylated gDMR in *Dnmt1* was located in spermatocyte- and somatic-specific exons, while oocyte-specific exons were hypo-methylated in oocytes (Figure S9). *Dnmt3L*$^{-/-}$ oocytes also showed hypomethylation in most of these gDMRs. Significant changes in the expression levels of genes with alternative splicing patterns were not observed in the *Dnmt3L*$^{-/-}$ oocyte genome (Figure 3, Figure 5E, and Figure S9). These results indicate that these oocyte-specific methylated gDMRs do not regulate gene expression or alternative splicing during the oocyte stage.